

**Recycled Aggregate Concrete immunized with Bagasse  
Carbonized Nano/Micro Particles against Freeze-Thaw  
resistance**



*Submitted by*

**Mansoor Lizan Ahamed**

Fall 2021-MS Structural Engineering

Reg. No: 00000397874

*Supervisor*

**Dr. Hammad Anis Khan**

**NUST INSTITUTE OF CIVIL ENGINEERING (NICE), SCHOOL OF  
CIVIL AND ENVIRONMENTAL ENGINEERING (SCEE), NATIONAL  
UNIVERSITY OF SCIENCES AND TECHNOLOGY (NUST),  
SECTOR H-12, ISLAMABAD, PAKISTAN**

This is to certify that the  
Thesis titled

**Recycled Aggregate Concrete immunized with Bagasse Carbonized Nano/Micro  
Particles against Freeze-Thaw resistance**

submitted by

Mansoor Lizan Ahamed

MS Structures 2021(00000397874)

has been accepted towards the partial fulfilment of  
the requirements for the degree

of

**MASTER OF SCIENCE**

**in**

**STRUCTURAL ENGINEERING**

---

Dr. Hammad Anis Khan

Structural Engineering Department,

NICE, SCEE NUST, Islamabad, Pakistan


# THESIS ACCEPTANCE CERTIFICATE

It is certified that final copy of MS thesis written by Mr. Mansoor Lizaḥ Ahamed, Registration No. 00000397874, of MS Structural Engineering batch 2021 (NICE), has been vetted by undersigned, found completed in all respects as per NUST Statutes/Regulations, is free of plagiarism, errors, and mistakes and is accepted as partial fulfilment for award of MS degree.

Signature: 

Supervisor: Dr. Hammad Anis Khan

Date: 3/8/2023

Signature (HoD): 


**HoD Structural Engineering**

NUST Institute of Civil Engineering

School of Civil & Environmental Engineering

National University of Sciences and Technology

Date: 3/8/2023

Signature (Principal & Dean): 

Date: 03 AUG 2023

**PROF DR MUHAMMAD IRFAN**  
Principal & Dean  
SCEE, NUST

## **CERTIFICATE**

Certified that the contents and form of the thesis entitled

**“Recycled Aggregate Concrete immunized with Bagasse Carbonized Nano/Micro  
Particles against Freeze-Thaw resistance”**

Submitted by

**Mansoor Lizan Ahamed (00000397874)**

Has been found satisfactory for partial fulfillment of the requirements of the degree of  
Master of Science in Structural Engineering

**Supervisor** \_\_\_\_\_

**Dr. Hammad Anis Khan**

**Assistant Professor, NICE, SCEE, NUST**

**GEC Member** \_\_\_\_\_

**Dr. Muhammad Usman**

**HOD structure, NICE, SCEE, NUST**

**GEC Member** \_\_\_\_\_

**Dr. Junaid Ahmad**

**Assistant Professor, NICE, SCEE, NUST**

**GEC Member** \_\_\_\_\_

**Dr. Ather Ali**

**Assistant Professor, NICE, SCEE, NUST**

## **DECLARATION**

I certify that this research work titled “Recycled Aggregate Concrete Immunized with bagasse Carbonized Nano/Micro Particles against Freeze- Thaw resistance” is my own work. The work has not been presented elsewhere for assessment. The material that has been used from other sources has been properly acknowledged /referred.

---

MANSOOR LIZAN AHAMED

2021-NUST-MS-STR-00000397874

MS Structural Engineering 2021 Batch (NICE)

## ACKNOWLEDGEMENT

I express my gratitude to Allah for His blessings and the strength he has granted me, enabling me to successfully accomplish this thesis. I am deeply grateful to my parents, whose prayers and inspiring actions have always been instrumental in my personal growth and accomplishments. I am extremely grateful to my thesis supervisor, Dr. Hammad Anis Khan, and Dr. Rao Arsalan khushnood for their valuable guidance, insightful advice, and attentive supervision.

I would like to extend my gratitude to all the technicians and office staff of the Department of Structural Engineering at NICE for their kind cooperation. I am also thankful to the lab assistants in the Geotechnical Lab at NICE and the Transportation Lab at NIT for their support during the preliminary tests. I would like to express my appreciation to the Lab Engineers of the XRD, FTIR, and SEM labs at SCME for their assistance with the XRD, FTIR, and SEM analyses, respectively. And also, I would like to thank the staff of the TGA lab at SMME for their cooperation in providing access to the TGA testing facility. Lastly, I would like to express my gratitude to friends and colleagues, particularly to Engr. Mohamed Ramsin Rayeesulhaq for their unwavering support throughout my research journey.

## ABSTRACT

Concrete is the most consumed material all over the world in construction industry. Recently, sustainable development and environmental awareness have become important attributes of societal growth. Waste concrete, which derives from the demolition of old concrete structures, is one of the most important construction wastes, alongside durability of concrete is main issue nowadays and different materials are added to concrete to improve especially against frost actions. Nanotechnology has revolutionized the field of materials and present a great opportunity to improve the properties of concrete via successive nano-scaled modifications. Moreover, use of nano-waste particles contributes to add into effectiveness as ecofriendly concrete. Mitigation of nano-flaws will render concrete more robust to be used in environment where it is generally avoided. In this research, CNMPs is induced into cementitious mix to make it more resilient in harsh conditions. Bagasse CNMPs were obtained from bagasse sugarcane by pyrolysis process and the characterizations were tested successfully. Five different dosages of bagasse CNMPs by mass of cement, 0.2%, 0.4%, 0.6%, 0.8% and 1% were induced in Recycled Course Aggregate concrete and its effect on frost resistance, acid attack, chloride migration, microstructure, porosity, compressive strength in comparison to control sample were studied. Test result shows that concrete was still durable after 7,14,21 and 28 freeze-thaw cycles. Freeze-thaw response was evaluated from scaling and internal structure damage and freeze-thaw resistance was improved. Scanning electron micrographs have verified the crack branching and crack bridging effects of induced bagasse CNMPs. Bagasse CNMPs may offer nucleation sites for hydration products (CSH gel) which make the microstructure dense and impermeable. Compressive strength before and after freeze-thaw exposure was determined and was enhanced with addition of CNMPs. Scaling effect of acid attack was reduced with increase in CNMPs content. Addition of CNMPs has improved chloride permeability resistance of the matrix. Reduction in porosity and making the mix impermeable due to addition of CNMPs was also verified from BET test results.

# CONTENTS

<b>CONTENTS.....</b>	<b>1</b>
<b>CHAPTER 1 .....</b>	<b>1</b>
1 INTRODUCTION .....	1
1.1 General.....	1
1.2 Bagasse Bio Char.....	3
1.3 Research Significance.....	4
1.4 Thesis Outline .....	4
<b>CHAPTER 2 .....</b>	<b>6</b>
2 LITERATURE REVIEW .....	6
2.1 General.....	6
2.2 Previous studies on Recycled Coarse Aggregate concrete.....	6
2.3 Previous studies on remedial measures of RCA concrete.....	9
2.4 Microstructure of nano-modified cementitious matrix .....	11
2.5 Porosity reduction in nano-modified cementitious composites .....	11
2.6 Review of nano induced RCA concrete.....	13
2.7 Concrete durability.....	14
<b>CHAPTER 3.....</b>	<b>17</b>
3 EXPERIMENTAL PROGRAMS.....	17
3.1 General.....	17
3.2 Concrete Materials .....	17
3.2.1 Cement.....	17
3.2.2 Sand .....	17
3.2.3 Recycled Coarse aggregate.....	18
3.3 Production of CNMPs and Characterization.....	19
3.3.1 Bagasse .....	19
3.3.2 Pyrolysis.....	19
3.3.3 Bagasse Carbon Nano/Micro Particles .....	21
3.4 Characterizations of bagasse CNMPs .....	21
3.4.1 Particle Size Distribution (PSD) .....	21
3.4.2 Scanning Electron Microscopy and Energy Dispersive X-ray spectroscopy.....	21
3.4.3 X-Ray Diffraction (XRD).....	22
3.4.4 Thermal Gravimetric Analysis (TGA) .....	22
3.4.5 Fourier Transform Infrared (FTIR).....	22
3.5 Mix proportions and preparation of CNMP's reinforced concrete samples .....	22
3.6 Freeze-thaw testing .....	24
3.6.1 Scaling .....	24
3.6.2 Freeze- thaw Internal structure damage.....	26
3.6.3 Compression test before and after freeze-thaw cycles.....	26
3.7 Acid attack: .....	27
3.8 Chloride migration test: .....	27
3.9 Microstructural investigation .....	29
<b>CHAPTER 4.....</b>	<b>30</b>
4 RESULTS AND DISCUSSION.....	30



4.1	Characterization of bagasse CNMPs .....	30
4.1.1	Particle Size Distribution (PSD) .....	30
4.1.2	Scanning Electron Microscopy (SEM) and EDX .....	31
4.1.3	X-Ray Diffraction (XRD) .....	32
4.1.4	Fourier Transform Infrared Spectroscopy (FTIR) .....	33
4.1.5	Thermal Gravimetric Analysis (TGA) .....	34
4.2	Freeze-thaw testing in concrete.....	35
4.2.2	Freeze-thaw internal structure damage .....	37
4.2.3	Compression test before and after freeze-thaw cycles.....	38
4.3	Acid attack in concrete.....	40
4.4	Chloride migration test in concrete .....	41
4.5	BET Porosimetry in concrete .....	42
<b>CHAPTER 5</b>	<b>.....</b>	<b>44</b>
5	CONCLUSIONS AND RECCOMENDATIONS .....	44
5.1	Conclusions.....	44
5.2	Recommendations .....	45
<b>CHAPTER 6</b>	<b>.....</b>	<b>46</b>
REFERENCES	.....	46

## LIST OF ABBREVIATIONS

CNMPs	Carbonized Nano/Micro Particles
ITZ	Interfacial Transition Zone
NCA	Natural Coarse Aggregates
GNMPs	Graphite nano/micro platelets
MIP	Mercury Intrusion Porosimetry
RCA	Recycled Concrete Aggregate
PSD	Particle Size Distribution
PSA	Particle Size Analyzer
FTIR	Fourier Transform Infrared Spectroscopy
SEM	Scanning Electron Microscopy
XRD	X-Ray Diffraction
TGA	Thermal Gravimetric Analysis
UPV	Ultrasonic Pulse Velocity
C-S-H	Calcium-Silicate-Hydrate
CH	Calcium Hydroxide
OPC	Ordinary Portland Cement
ASTM	American Society for Testing and Materials
CNTs	Carbon Nano Tubes
CNFs	Carbon Nano Fibers

## LIST OF FIGURES

Fig. 2. 1. Optical (1) and SEM (2) images of NCA & RCA: (a) NCA; (b) RCA .....	7
Fig. 2. 2. Compressive strength of concrete with respect to different % of RCA.....	8
Fig. 2. 3. Compressive and shear strength of RCA and NA concrete .....	9
Fig. 2. 4. MIP analysis of modified cement paste .....	12
Fig. 2. 5. MIP analysis showing cumulative pore volume .....	12
Fig. 3. 1. (a) Sun Dried Bagasse (b) Ground Bagasse (c) Iron Dried Bagasse .....	20
Fig. 3. 2. (a) Pyrolysis set up (b) Schematic Diagram of Pyrolysis .....	20
Fig. 3. 3. (a) Ground Bagasse (b) Biochar (c) Hand Grinding of Biochar .....	21
Fig. 3. 4. (d) Planetary ball milling of biochar (e) Milled Biochar (CNMPs).....	21
Fig. 3. 5. (a) The test arrangement of slab test (b) Sample prepared .....	25
Fig. 3. 6. Specimen (a) before sulfate attack (b) after sulfuric attack.....	27
Fig. 3. 7. Chloride Migration Test.....	29
Fig. 4. 1. Particle size distribution of bagasse CNMPs .....	30
Fig. 4. 2. (a) SEM image of bagasse CNMP sheets (b) Nano Particles embedded in sheets .....	31
Fig. 4. 3. EDX Spectra of bagasse CNMP .....	31
Fig. 4. 4. X-Ray Diffraction pattern of CNMPs.....	33
Fig. 4. 5. FTIR spectra of CNMPs .....	33
Fig. 4. 6. TGA plot of biochar.....	34
Fig. 4. 7. Freeze-thaw scaling .....	36
Fig. 4. 8. SEM images of (a) 0%CNMP's (b) 1%CNMP's before freeze-thaw cycles.....	37
Fig. 4. 9. Internal structure damage .....	38
Fig. 4. 10. Scanning electron microscopy of (a) 0%CNMP's (b) 1%CNMP's after frost attack.....	38
Fig. 4. 11. Comparison of compressive strength before and after freeze-thaw cycles.....	39
Fig. 4. 12. Sulfate attack scaling at 14 and 28 days exposure.....	40
Fig. 4. 13. Chloride migration co-efficient .....	42
Fig. 4. 14. Nitrogen absorption isotherm (a) before (b) after frost attack.....	43

## LIST OF TABLES

Table 2- 1: MIP analysis nano modified cement pastes .....	11
Table 2- 2: Porosity of sample with GNP and CHS .....	13
Table 3- 1: Chemical composition of OPC used in the proposed formulation. ....	17
Table 3- 2. Physical properties of fine aggregate .....	18
Table 3- 3. Physical and mechanical properties of recycled coarse aggregate.....	18
Table 3- 4: Composition of concrete samples .....	23
Table 3- 5: No. and size of samples prepared from each batch.....	23
Table 3- 6: Time and temperature maintained during freeze-thaw cycle. ....	26
Table 4- 1: Composition of bagasse CNMP .....	32
Table 4- 2: Penetration depth and migration co-efficient.....	42

# 1 INTRODUCTION

## 1.1 General

Concrete is considered as the widely used construction material globally[1]. It is a composite material consisting of multiple phases, with its properties derived from its component materials, namely cement, fine aggregates, coarse aggregates, and water. Due to the increasing demand and upgrading of infrastructure, the use of concrete has gradually increased, depleting natural resources due to the excessive use of natural coarse aggregates(NCA). Meanwhile, a significant amount of waste is produced annually, and the majority of it is disposed off in landfills or suburban areas, causing environmental contamination and taking up space. The majority of the amount of concrete is made up of coarse aggregates, which make up the majority of the materials[2]. As a result, there is a high demand for coarse materials in construction. The construction industry has used a significant quantity of raw materials and produced a considerable amount of waste from construction and demolition since the beginning of the twenty-first century due to the fast urbanization and industrialization.

Recycled aggregate concrete (RAC) has gained attention as a solution to address the issue of environmental degradation and the increase in waste from construction and demolition activities. Recycled concrete aggregate (RCA) made from the refuse of buildings and demolition to create RAC. Research into RCA properties and their use in concrete started more than 30 years ago[3]. The majority of previous trials, however, were restricted to non-structural grade RAC because of the undesirable physical properties of RCA, such as high water absorption, which leads to higher water consumption for a given workability. Nevertheless, in contemporary times, RCA can be used to create solid concrete that is high-strength and high-performing. The mix composition and general properties of concrete are influenced by the structural characteristics of RCA.

Recycled aggregate often has inferior physical characteristics such as form, texture, specific gravity, bulk density, pore volume, and absorption due to the presence of cement paste/mortar and impurities. This implies that the efficacy of the resulting concrete is greatly influenced by the quality of the aggregates used. Researchers have suggested various methods to enhance the performance of recycled aggregate concrete, such as

eliminating or strengthening the related cement. The microstructure of concrete is a key determinant of its performance, and enhancing the microscopic properties of RAC can lead to improved macroscopic properties as well.

Natural aggregate and cement slurry are combined to create recycled concrete aggregate (RCA), which has an interfacial transition zone (ITZ) that serves as a transitory phase between the cementitious substance and natural aggregate. A composite substance known as RAC is produced in concrete when RCA is used to substitute all or part of the natural aggregate. RAC is made up of three ITZs: NA-Old mortar ITZ, NA-New mortar ITZ, and new mortar-Old mortar ITZ. The ITZ is composed of three layers: a layer of water, a layer of calcium hydroxide (CH) crystals, and a layer of permeable paste matrix. It is the weakest phase in RAC, and it significantly impacts the concrete's strength and lifespan. Two fracture toughness indices - ITZ-3, which determines the water-binder ratio when it is high, and ITZ-2, which determines the water-binder ratio when it is low—determine the compressive strength of RCA concrete.

When cement contains a large amount of calcium silicate and calcium aluminate, the initial hydration stage results in the formation of more  $\text{Ca}(\text{OH})_2$  and ettringite crystals, which adhere to the surface of RCA. This process alters the RCA surface's porosity and weakens the RAC microstructure, affecting its properties. During subsequent hydration stages, various C-S-H gels and  $\text{Ca}(\text{OH})_2$  crystals are formed, and the quantity of ettringite crystals and pores reduces, resulting in a uniform and compact RAC microstructure[4]. Improving the microstructure and properties of RAC can be achieved by modifying the microstructure of RCA and ITZs because RCA's structure is associated with ITZs and porosity.

{The use of nanomaterials has been demonstrated to be a viable and efficient method for addressing the limitations of recycled aggregate concrete (RAC). Studies have looked at how RAC's workability, tensile strength, durability, and dimensional stability are affected by the inclusion and alteration of nano-materials. In microstructural studies, researchers have focused on the impacts of nano-modification on the interfacial transition zone (ITZ). The findings show that adding nanomaterials usually decreases the workability of RAC, speeds up cement hydration, and enhances the mechanical properties and endurance of the cement. However, there are some differences in the types, quantities, and alteration methods of the nanomaterials used. The nucleation effect, filling effect, pozzolanic effect, bridging effect, and increase of ITZs are the main mechanisms for how effectively RAC

is modified with nanoparticles. The effects of using nanomaterials in RAC are also quickly assessed in terms of their economical and environmental effects[4]. Concrete is a versatile building material that offers strength, durability, and cost-effectiveness in construction. However, it is vulnerable to damage from freeze-thaw cycles, which can cause scaling and internal structural damage. The strength, lifespan, and safety of conventional cement-based materials can be further compromised by their poor tensile strength and tendency for cracking[5]. The formation of internal cracks caused by freeze-thaw cycles can be avoided by adding various kinds of microfibers to the matrix, which can also enhance the mechanical and durability characteristics of cement-based materials. Additionally, nano reinforcements may prevent the initiation and development of nanoscale cracks as well as their spread to the microscale[6]. Nanoscale fibers can prevent the emergence of microcracks at the nanoscale due to their increased strength and stiffness, bigger aspect ratio, and reduced fiber spacing[7]. Concrete that contains nanoparticles is more likely to be more resilient, self-healing, microstructurally thick, and compress more quickly[8].

Several techniques, including forming voids to allow water growth during freezing and increasing microstructure to hinder water entry, can be used to increase frost resistance[9]. A popular technique for increasing frost resistance is air entrainment, but it has some technological problems with ordinary concrete like air bubble merging during mixing and air loss during pumping. Carbonized Nano/Micro Particles (CNMPs) can be used as a resource to alter the porous structure of cementitious systems in traditional concrete. Total porosity and the length of the induction phase both diminish when CNMP is added to the mixture. The quantity of water in the concrete is significantly reduced as a consequence of the mix's diminished permeability[10][11]. By reducing the amount of water, the osmotic pressure caused by water and damage caused by freezing water are both reduced. Due to the shape of CNMPs, microcracks can be blocked and rerouted delaying the spread of fractures.

## **1.2 Bagasse Bio Char**

Bagasse, a byproduct from sugarcane processing, is typically discarded or burned, which adds to pollution. One ton of sugarcane produces about 280 kg of bagasse, according to agricultural studies[12]. Finding a use for this material is essential to reducing pollution and CO<sub>2</sub> emissions. One solution is to use pyrolysis, a process that can yield solid, liquid,

and gaseous fuels from bagasse. To enhance the tensile, thermal, electrical, and chemical characteristics of cementitious systems, the solid substance known as biochar can be used[13].

According to the literature currently available, adding different nanomaterials to concrete, such as CNMPc, carbon nanotubes, nanoclay, and nanosilica, may improve its characteristics. The current study focuses on the potential impact of CNMPs on RCA concrete.

### **1.3 Research Significance**

Freeze-thaw cycles may lead to scaling and damage to the internal structure of concrete, especially when exposed to deicer salt. However, there have been comparatively few studies on the application of nanomaterials to enhance freeze-thaw resistance in recycled aggregate concrete, despite the fact that many scholars are looking into methods to address this issue. (RAC). Waste concrete is crushed during RAC manufacturing, which may cause microscopic fractures in the aggregate. The possible technical uses of RAC can be increased by incorporating nanomaterials, and this will support sustainable growth in the building sector. CNTs, CNFs, graphene, graphene oxide, and GNMPs are examples of carbon-based nanoparticles that can be used to create nano-modified concrete and increase RAC's frost protection[14].

As an affordable and accessible option to other carbon nano inclusions, this study uses nanosized agricultural and industrial waste carbon.

### **1.4 Thesis Outline**

This study is consisting of five chapters and outlines the objectives and significance of the research being conducted.

Chapter 1: “Introduction” – this study provides an initial overview of how Nano modified RAC behaves when subjected to freeze-thaw conditions particles. Similar to other carbon-based compounds, carbon biochar has characteristics that facilitate hydration through the nucleation effect and its high specific surface area. The performance of RAC is effectively altered by the inclusion of CNMPs, eventually delaying the formation of cracks and enhancing its freeze-thaw resistance.



Chapter 2: “Literature Reviews” – this chapter provides an extensive analysis of previous studies conducted on the properties of CNMPs and RCA when incorporated into concrete, as well as their response to freeze-thaw cycles.

Chapter 3: "Experimental Methodology" – is a chapter that outlines the testing procedures and equipment used to evaluate the mechanical properties of the specimens. The chapter provides a comprehensive description of the test setup, including the methods used to measure different properties.

Chapter 4: This section presents an analysis and discussion of the material property tests. It includes the results of the freeze-thaw tests and microstructural study, as well as the presentation of simple linear empirical freeze-thaw relationships of modified mixes. The section also discusses the results of chloride migration and acid attacks in detail and presents them in empirical graphs.

Chapter 5: “Conclusions and Recommendations” – The findings from the results are presented in the conclusion section.

References have been provided at the end.

### 2 LITERATURE REVIEW

#### 2.1 General

The use of recycled aggregates (RCA) in place of natural aggregates (NA) in concrete as well as the use of carbon-based nanomaterials to strengthen the concrete properties, particularly in terms of freeze and thaw resistance, will be addressed in this chapter. For all types of concrete, especially in cold climates, freeze-thaw resistance is an essential quality[9]. Water expands and adds around 9% additional volume as it freezes. This applies tensile stress to the nearby concrete, which, if the tensile stress exceeds the material's resistance, may result in scaling, cracking, and eventually degradation. The repeated cycle of freeze-thaw activity can seriously degrade the concrete structure and perhaps lead it to collapse.

Numerous global research projects are now aimed at improving the freeze-thaw resilience of traditional concrete structures. So far, no studies have been undertaken regarding the use of CNPns to improve the freeze-thaw resistance of RCA concrete systems.

#### 2.2 Previous studies on Recycled Coarse Aggregate concrete

The efficient use of recycled coarse aggregate (RCA) in concrete has been the subject of several studies, and some of the key researches pertinent to the current topic are provided here. A mechanical investigation on recycled coarse aggregate made from demolished structures was carried out[15]. To obtain the same strength for all mixtures, the replacement percentages of recycled aggregate were kept at 0%, 25%, 50%, and 100%. Concrete was employed with RCA in a moist but not saturated state to keep its fresh properties. The results showed that, due to the weaker mortar used to attach the aggregate to the mix, the 100% RCA replacement mix had a compressive strength that was 20% lower than that of virgin coarse aggregate concrete made with the same water to binder ratio and cement content. To attain the same strength, though, more cement is needed. The study also discovered that medium strength concrete with 30-45 MPA and 25% RCA substitution had strength comparable to that of natural concrete. Additionally, it was shown that RCA concrete had a greater split tensile strength than regular coarse aggregate concrete. The failure mechanisms of RCA concrete were also explored in the study. To

explain, the Interfacial Transition Zone (ITZ), which is often the most fragile region in traditional concrete, is the cause for failure. For recycled coarse aggregate (RCA) concrete, this is not the case. RCA concrete failure, which happens through the aggregates themselves, is more comparable to high-strength concrete failure. According to the findings of the split tensile strength tests conducted in this research, the failure in RCA concrete happened via the aggregates.

By employing regularly recycled coarse aggregates to create structural concrete, seek to solve environmental, economic, and social challenges[16]. To evaluate the effects of recurrent usage of RCA, the researchers conducted laboratory trials in which RCA was used to replace 100% of the typical coarse aggregates. However, even after numerous cycles, the RCA concrete still satisfied the structural criteria. The results showed that RCA usage in concrete repeatedly decreased its strength and increased chloride penetration. The ITZ was credited for the instability in the RCA concrete's toughness. The ITZ in RCA consists of more than one bonding, including old mortar, old aggregate bond, and old mortar new mortar bonding, which lowered its strength. In contrast, the ITZ in natural coarse aggregate concrete is formed of new mortar and fresh virgin aggregates. Fig. 2.1 shows SEM images of natural and RC aggregate. According to the study, concrete may be made to be structurally sound and have a lifespan of 50 years by employing 100% RCA.

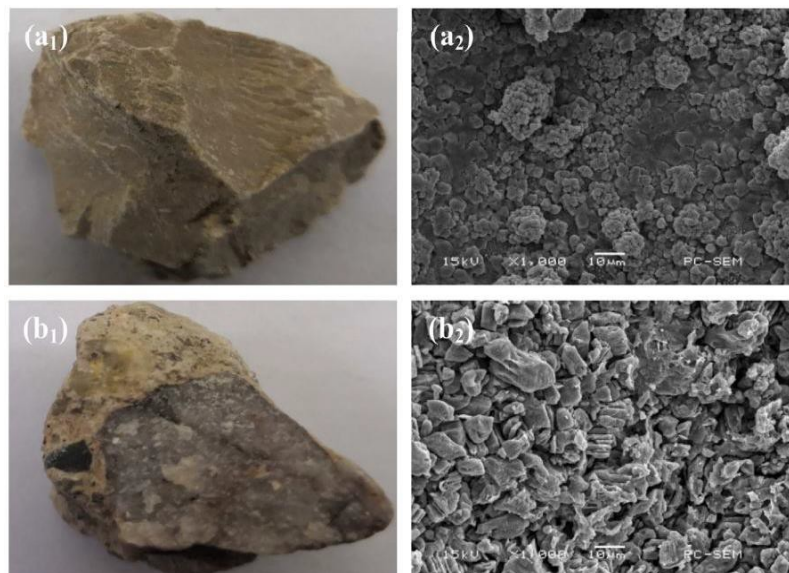


Fig. 2. 1. Optical (1) and SEM (2) images of NCA & RCA: (a) NCA; (b) RCA

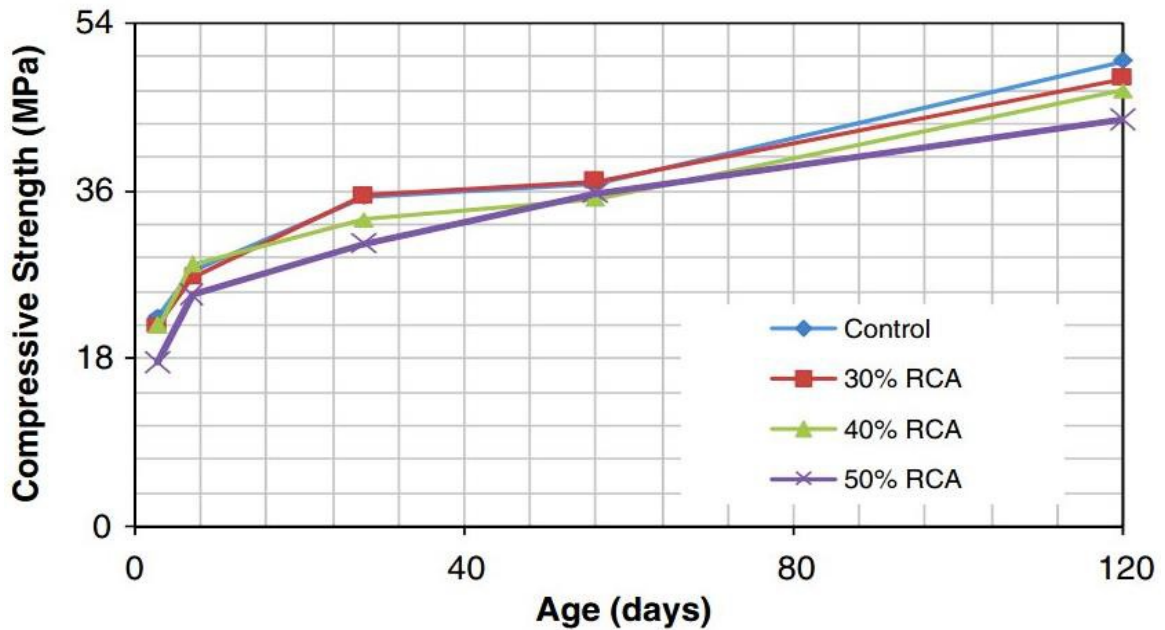


Fig. 2. 2. Compressive strength of concrete with respect to different % of RCA

In order to determine how recycled coarse aggregate affected the characteristics of both freshly poured concrete and hardened concrete, performed a research. At curing ages of 3, 7, 28, 56, and 120 days, the mechanical characteristics of specimens with a strength of 35 MPA were examined[17]. The RCA replacement ranged from 0% to 50%. The results showed that RCA concrete performed similarly to natural coarse aggregate concrete overall but had a small drop in compressive strength. The correlation of compressive strength at various RCA % is shown in Fig. 2. 2.

The characteristics of concrete incorporating recycled coarse aggregates and natural coarse aggregates were compared[15]. Ten mixtures total comprising virgin and recycled aggregates were used in the study, with strengths ranging from 20 MPA to 50 MPA. To study compressive and shear strength, a variety of specimens, including cubes, were tested at curing ages of 7, 14, 28, and 56 days. A variety of cylindrical samples were also examined at a curing age of 28 days to look at mechanical characteristics including the maximum compressive strength and elastic modulus.

Recycled coarse aggregate concrete demonstrated, for the same mix percentage, an average of 90% of the compressive and shear strength of natural aggregate concrete at a curing age of 28 days[15]. Concrete using recycled coarse aggregates and a strength range of 25 MPA to 30 MPA produced cylindrical specimens with an elasticity modulus that was 3% lower than concrete manufactured with virgin aggregates. Similar patterns could

be seen in the compressive strength, shear strength, and strain of concrete made using recycled coarse aggregate and unreinforced concrete. Below Fig. 2. 3 compare the compressive strength and shear strength of the two varieties of NA and RAC concrete at a curing age of 28 days.

### 2.3 Previous studies on remedial measures of RCA concrete

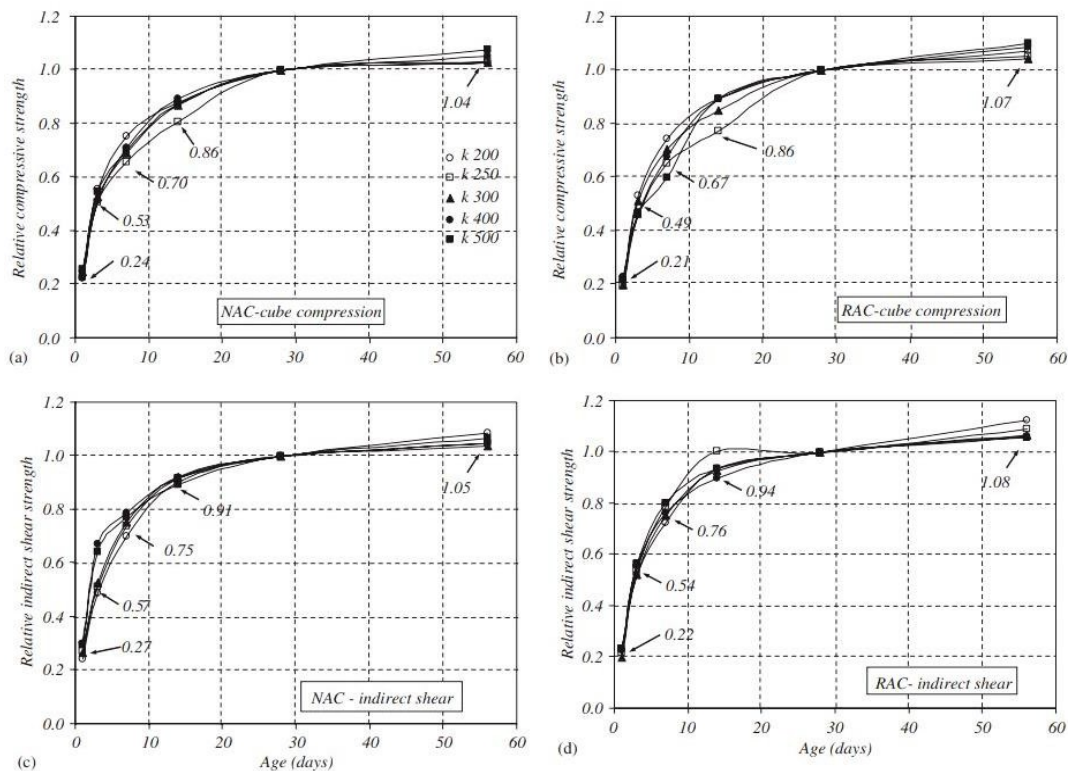


Fig. 2. 3. Compressive and shear strength of RCA and NA concrete

Numerous research studies have been conducted to identify ways to overcome the drawbacks of recycled coarse aggregate (RCA) concrete, including the use of mineral and chemical admixtures. In this area, some of the pertinent researches are included:

The features of recycled coarse aggregate concrete with the inclusion of a chemical additive that has water repellent qualities and can enhance workability were studied[18]. RCA loses workability because it tends to absorb more water while mixing since it has increased porosity. In order to explore compressive strength, tensile strength, and flexural strength qualities, the study entailed casting cubes with dimensions of 150 x 150 x 150 mm, cylinders having diameter of 150 mm and length of 100 mm, and beams having dimensions of 100 x 100 x 500 mm.

According to the results, the application of a chemical additive in RCA concrete increased

its workability by lowering its porosity, approaching that of concrete made with natural coarse aggregate. The compressive strength of specimens made with 20% recycled coarse aggregate and 150 ml of the chemical admixture was nearly identical to that of control specimens, demonstrating that the chemical admixture had improved the weak interfacial transition zone.

The addition of a waterproofing admixture was examined to assess its impact on the compressive strength and water penetration of RCA aggregate[19]. The admixture was added to the mixture, and parameters such air content, water absorption, density, and compressive strength were assessed in both the fresh and hardened phases of the combination. The outcomes revealed that the admixture's inclusion increased the concrete's workability by encouraging proper cement particle dispersion and releasing water between them.

The effects of various mineral admixtures, including silica fume, fly ash, and ground granulated blast slag, on the characteristics of RCA concrete were investigated[20]. The specimens utilised in this investigation comprised 75mm x 75mm x 285mm prisms to analyse tensile strength, drying shrinkage, and chloride penetration, 100mm diameter and 150mm cubes to assess compressive strength, 100mm diameter and 200mm height cylinders, and 100mm diameter and 200mm height cylinders. According to the study, the concrete's temperature was essentially the same with and without the waterproofing ingredient, and the mixture's density, which ranged from 2300 to 2400 Kg/m<sup>3</sup>, was also similar. In comparison to RCA mix, RAC with a waterproofing agent had less chloride penetration.

Additionally, the study discovered that the use of 100% recycled coarse aggregate (RCA) and silica fume in concrete led to increased strength properties. Mineral additive, which boosted bonding strength between new mortar and old RCA by strengthening the interfacial transition zone, can be credited for this improvement. A mineral admixture was also added, which led to an increase in ultrasonic pulse velocity (UPV) and a decrease in chloride penetration in the combination, taking into account the high porosity of RCA. The study found that although fly ash only improved the durability features of concrete, silica fume boosted both its strength and lifespan characteristics.

## 2.4 Microstructure of nano-modified cementitious matrix

Concrete composed of nanomaterials has a more compact microstructure and less porosity as they work as a filler and reinforcement at the same time[21]. Enhanced mechanical characteristics result from the improved microstructure. In the presence of fly ash, carbon nanotubes (CNTs) occupy the spaces left by the hydration of materials such as ettringite and calcium silicate hydrate (CSH) gel[22]. The composite's improved strength is a result of the addition of CNTs and fly ash. CNTs successfully transmit loads in the form of tensile strains via fractures in nano-modified concrete[23]. By creating a solid connection with the cement matrix by the use of nanomaterials, the concrete is strengthened, resulting in improved mechanical properties and failure characteristics. The crack bridging mechanism improves the flexural strength of concrete enhanced with nanotechnology[24].

## 2.5 Porosity reduction in nano-modified cementitious composites

The porosity of the material is improved by evenly dispersing nanomaterials into cementitious composites. The microstructure is improved by a decrease in porosity and mesopores when the water-to-cement ratio (w/c) is 0.5 and the nanomaterials, namely 1wt.% carbon nanotubes (CNTs), are appropriately disseminated[25]. A mercury intrusion porosimetry test was carried out after nano-modified cement pastes had dried for 28 days, yielding information on the cement's overall porosity, total volume of mercury intrusion, and overall surface area. The porosity of the composites reduces as the quantity of multi-walled carbon nanotubes (MWCNTs) increases. Notably, the lowest intrusion and porosity are produced by the presence of 1% CNTs.

Table 2- 1: MIP analysis nano modified cement pastes

Mixes	Total intruded volume (cm <sup>3</sup> /g)	Total porosity (%)	Total surface area (m <sup>2</sup> /g)
PC	0.717	27.14	31.45
0.5% CNTs	0.1494	25.52	25.36
1% CNTs	0.1422	22.73	24.32

Mesopores (size  $\leq 50$  nm) and macropores (size  $\geq 50$  nm) are two different types of pores seen in Fig. 2. 4[26], where the presence of CNTs causes a decrease in macropores. Spreading MWCNTs in the mixture reduces porosity and encourages a uniform distribution of pores[27]. As shown in Fig. 2. 5 found that adding 0.25% CNTs reduces porosity without significantly impacting strength[28]. As shown in Table 2.6, graphene nanoplatelets (GNPs) also assist to reduce porosity and enhance other characteristics[29].

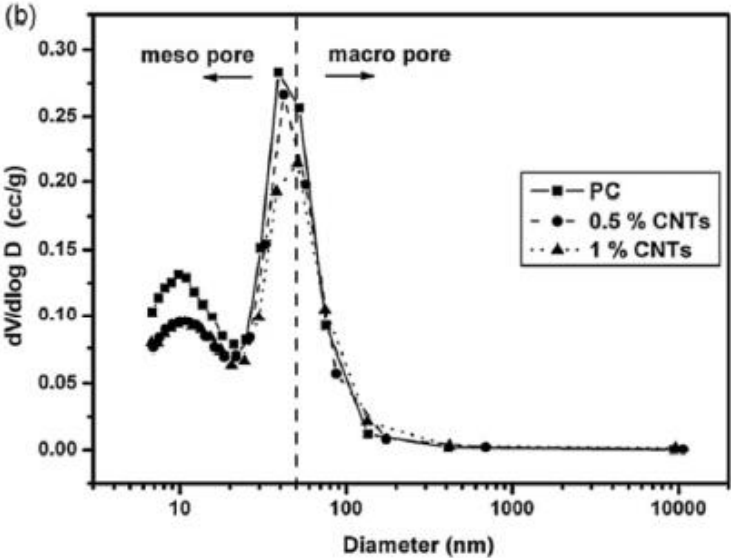


Fig. 2. 4. MIP analysis of modified cement paste

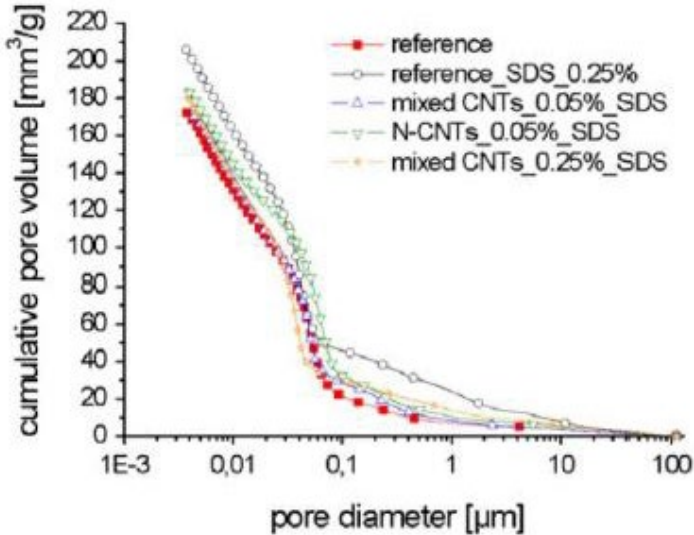


Fig. 2. 5. MIP analysis showing cumulative pore volume



Table 2- 2: Porosity of sample with GNP and CHS

Sample ID	Avg. Pore radius (nm)	Max. pore radius (nm)	Total porosity (%)	Porosity (%) (diameter ≤ 100nm)	Porosity (%) (diameter ≥ 100nm)
CEM	10.1	56741.5	17.4	69.4	30.6
0.2_GNPs_3	6.4	54651.2	12.54	82.54	17.8
0.2_GNPs_4	5.2	52564.1	11.48	84.51	15.4
0.2_CBF	7.2	56169.5	14.58	74.56	21.85
0.2_CHS	6.6	55742.4	14.42	77.52	18.74
0.2_CPS	6.5	54852.4	13.54	78.65	18.24

Numerous studies indicate that nano-modification improves pore size distribution, decreases porosity, and increases the strength of cementitious composites[30].

## 2.6 Review of nano induced RCA concrete

Numerous investigations have been conducted to address the drawbacks of RCA concrete, including the use of nano particles. In the following section, some of the relevant and noteworthy studies are outlined:

Due to their potential to improve the characteristics of concrete, nano-scale materials have drawn a lot of interest[31]. Materials' large surface area can have a considerable influence on the characteristics of concrete when they are reduced to the nanoscale in at least one dimension[32]. According to the literature, nano-silica (NS) and graphene oxide (GO) are the two nano-materials that are most frequently employed. Because of their high surface-to-volume ratio, which serves as crystal nuclei and improves cement hydration, nanoparticles have been frequently used in concrete. Several studies have shown that the addition of nano-materials may greatly enhance the early age attributes of concrete without affecting its long-term performance[33]. The study of the characteristics of nano-modified RAC has advanced significantly in recent years[34]. Controlling the behaviour of the material and achieving improved mechanical and durability features are the key goals of employing nano-materials in RAC. Nanomaterials have the potential to impact various stages of RAC's hydration and hardening processes[35]. Certain nano-particles can improve the morphology of both the matrix and the ITZs in RAC and refine the structure of C-S-H[36]. As a substitute for nanoparticles, one-dimensional nanomaterials like CNTs could improve the connection between hydration products and decrease microcracks[37]. Due to its oxygen-containing groups, GO, a two-dimensional

nanomaterial, may be readily disseminated in the matrix and exhibits high attractive forces similar to CNT[38]. The use of nano-materials provides a larger variety of technical applications for RAC and supports sustainable growth in the construction sector, in contrast to existing techniques for enhancing the qualities of either RA or RAC[39]. However, due to its high water absorption, poor dispersibility, and large specific surface area, directly combining nano-materials can reduce the workability of RAC. The cement hydration process in RAC is however facilitated by the presence of nanomaterials.

A lot of research shows that adding the right quantity of nanomaterials may improve the bond strength, flexural strength, splitting tensile strength, and compressive strength of RAC, but the ideal ratio of various nanomaterial kinds is still unknown[40]. On the other hand, there is little difference between nanomaterials and the elastic modulus of RAC. Depending on the materials and measurements used, different nanomaterials have different effects on the ductility of RAC[41]. In general, adding nanomaterials to RAC can increase its toughness by lowering water absorption and permeability and boosting its resistance to corrosion, acid, and freeze-thaw cycles.

The ideal quantity of nanomaterials to incorporate into RAC is still up for controversy, mostly because of the problem of agglomeration[42]. Bridging, pozzolanic reactions, nucleation, filling, and improvement of the ITZ are the key methods by which nanomaterials increase the mechanical and durability characteristics of RAC. The ITZ in RAC can be particularly improved by pre-spraying or pre-soaking the nanomaterials. ITZs in RAC have more complicated compositions and microstructures than those in NAC. Further investigation is required to establish links between the performance of RAC with introduced nanomaterials and the characteristics of ITZs at various levels in order to better understand the effects of nano-modification on RAC.

## **2.7 Concrete durability**

The freezing of interior moisture can cause frost damage to civil engineering infrastructure[36]. This causes internal cracking and internal frost attack as well as the removal of small particles from the surface of the concrete, a condition known as scaling[43]. Scaling is particularly noticeable in salt frost attack. According to sources [38][43], and[44], Powers et al.'s study largely examines the underlying ideas of freezing and thawing. According to these theories, the osmotic hypothesis says that dissolved substances cause water to migrate from unfrozen to frozen water, whereas the hydraulic

theory contends that water transfers from capillary pores to other pores. Litvan explained that water freezes close to the surface of concrete, while it remains unfrozen in capillary pores. When it moves, this cooled water may cause freeze-thaw damage. Air entraining chemicals are frequently utilised to improve the concrete's resistance to freeze-thaw. The addition of air content ranging from 4% to 8% is usually sufficient. However, concerns have been raised because adding more air to concrete to improve frost resistance weakens it.

According to several research investigations, increasing the density and impermeability of the microstructure can greatly increase durability against freezing and freezing[45] [46]. Studies on improving freeze-thaw resistance by adding nanomaterials to the cementitious matrix are few. In a study on the effects of several nano-materials on frost attack, Salemi et al. found that the presence of nanoparticles enhanced compressive strength and decreased water absorption in the mixture. Upon experiencing freeze-thaw cycles, concrete blends incorporated with nano-particles indicated reduced damage, reduced internal cracks, and increased strength. Carbon nanotubes (CNTs) were used in a study by Wang et al. to evaluate the freeze-thaw resilience of concrete[47]. When compared to conventional concrete, concrete mixtures incorporating CNTs showed a much greater resilience to freeze-thaw. Similar to this, Li et al. evaluated the resistance to frost attack of concrete mixes including CNTs and found increased resistance[48]. It is thought that adding CNTs to the mixture will have a bridging effect, lessen the amount of large pores, and reduce porosity. Furthermore, carbon fibres have been shown to be more favourable than CNTs in terms of reducing freeze-thaw damage[49]. The potential of carbon-based nanomaterials, in particular graphite platelets, was investigated in a study by Khushnood and Nawas to increase the cementitious matrix's resilience in adverse weather. The study looked at the results of adding different amounts of graphite nano/micro platelets to regular concrete (0.25%, 0.50%, 0.75%, and 1.0% by mass of cement). The major goal was to determine how these additives affected the concrete's salt freeze-thaw resistance by matching the results with a reference sample. According to the test findings, the concrete samples showed endurance even after 7, 14, and 28 freeze-thaw cycles. Surface scaling and inside structural damage were included in the evaluation of salt freeze-thaw performance, and both of these factors were improved with the addition of nano graphitic plates. The presence of these extra platelets caused crack branching effects, which were visible in scanning electron micrographs. The refinement in the pore structure, as shown

by nitrogen absorption isotherms, was attributed to the nano-modifications, increasing the concrete's resistance to damage from frost.

The impact of carbon nanotubes, graphene nanoplatelets (GNMPs), and other nanomaterials on freeze-thaw performance in ordinary concrete have been the subject of several investigations. However, the usage of CNMPs in relation to freeze-thaw resistance has not been studied. Our goal in this study is to assess CNMP's potential to improve the mechanical and durability characteristics of concrete mixes including recycled aggregate (RCA). There are several test procedures available to evaluate internal structural damage and freeze-thaw scaling in concrete.

**3 EXPERIMENTAL PROGRAMS**

**3.1 General**

This chapter's major goal is to provide an overview of the methods and processes used to achieve the intended results. In order to get the desired results, a thorough and complete explanation of the sequential procedure, beginning with the preparation of specimens and ending with the use of different testing techniques, has been given.

The choice of materials was primarily based on their availability. The growing significance of Nano Materials and Recycled Course Aggregate in the construction materials industry has led to their inclusion in this research. The materials used can be broadly classified into two categories: Nanotechnology and Construction Materials. In the field of Nanotechnology, nano particles were obtained using a pyrolyzing technique. On the other hand, the main construction material utilized was concrete, which was made with locally available Bestway cement. The locally sourced sand and coarse aggregates were obtained from tested cylindrical samples in the structure laboratory at NUST, H12 Islamabad, Pakistan.

**3.2 Concrete Materials**

**3.2.1 Cement**

Ordinary Portland Cement (OPC), which complies with ASTM C-150 specifications, was used as the binding material in the investigation. It had a 3.15 specific gravity (as reported by ASTM C-188) and a 3% fineness modulus (as calculated by ASTM C-430). The chemical characteristics of the binder are listed in Table 3-1.

Table 3- 1: Chemical composition of OPC used in the proposed formulation.

Compound	CaO	SiO <sub>2</sub>	Al <sub>2</sub> O <sub>3</sub>	Fe <sub>2</sub> O <sub>3</sub>	SO <sub>3</sub>	MgO	K <sub>2</sub> O
Percentages	<b>68.00</b>	<b>15.60</b>	<b>8.62</b>	<b>3.64</b>	<b>2.71</b>	<b>1.32</b>	<b>0.60</b>

**3.2.2 Sand**

Sand procured from the Lawrencpur area and that was in the saturated surface dry (SSD)

state was used as the experiment's fine aggregate. The sand was free of clay and other harmful substances. Table 3-2 has further information about the sand's physical attributes.

Table 3- 2. Physical properties of fine aggregate

Property	Fineness Modulus	Specific Gravity OD	Specific Gravity SSD	Apparent Specific Gravity	Water Absorption (Percentage)
ASTM Standard	C-136 [50]	C-128 [51]			
Values	2.64	2.70	2.76	2.85	2.35

### 3.2.3 Recycled Coarse aggregate.

Crushing tested cylinders with strengths ranging from 3000 to 4000 psi in the structural laboratory at NUST, Islamabad, Pakistan, produced the recycled concrete aggregate (RCA) used in the study. The mechanical and physical properties of the RCA are shown in Table 3. It was made from crushed cylinders that were between 9.5 mm and 12.5 mm in size. The RCA underwent a rigorous cleaning treatment before use.

In this study, all six mixes completely replaced natural materials with 100% recycled concrete aggregate (RCA). To guarantee compliance with requirements, this substitute needed to undergo extensive testing. Table 3.2 provides a list of the RCA's physical characteristics.

Table 3- 3. Physical and mechanical properties of recycled coarse aggregate

Property	ASTM Standard	Values
Fineness Modulus	C-136 [50]	7.51
Specific Gravity (OD)	C-127 [52]	2.12
Specific Gravity (SSD)		2.30
Apparent Specific Gravity		2.46

Water Absorption (Percentage)		6.15
Crushing Strength Value (Percentage)	IS 2386 Part IV [53]	24.20
Impact Value (Percentage)		23.14
LOS Angeles Abrasion (Percentage)		24.6

### 3.3 Production of CNMPs and Characterization

#### 3.3.1 Bagasse

The bagasse underwent a three-day sun-drying procedure after being purchased from a neighborhood juice bar. After that, it was processed in an electric grinder to a size that ranged from 0.4 to 1.8 mm. smaller particles, which are known to be superior in this respect, are the reason why this specific size range was chosen to enable appropriate temperature distribution during pyrolysis. Following grinding, the bagasse was further dried for three hours at 110°C in an oven to guarantee that all moisture had completely evaporated. Fig. 3. 2 provides an illustration of this procedure.

#### 3.3.2 Pyrolysis

Three useful byproducts are produced by the thermochemical process known as pyrolysis, which includes bio char, bio oil, and bio gases[54]. The selected technique is thoroughly described in the next section. The pyrolysis reactor was first filled with 200 grams of crushed and dried bagasse fibres as the feedstock. It was essential to entirely remove all oxygen from the assembly after starting the machine since pyrolysis only takes place without the presence of oxygen. A flow of nitrogen gas (N<sub>2</sub>) was injected for the first 30 minutes at a rate of 300 ml/min to guarantee the removal of oxygen. Once the temperature hit 500°C, which happens to be the region at which bagasse degradation is known to occur[55], the nitrogen gas supply was then maintained at 50 ml/min. 20°C/min of heating was applied. After reaching 500°C, the temperature was held there for 30 minutes before descending steadily but more slowly.



Fig. 3. 1. (a) Sun Dried Bagasse (b) Ground Bagasse (c) Iron Dried Bagasse

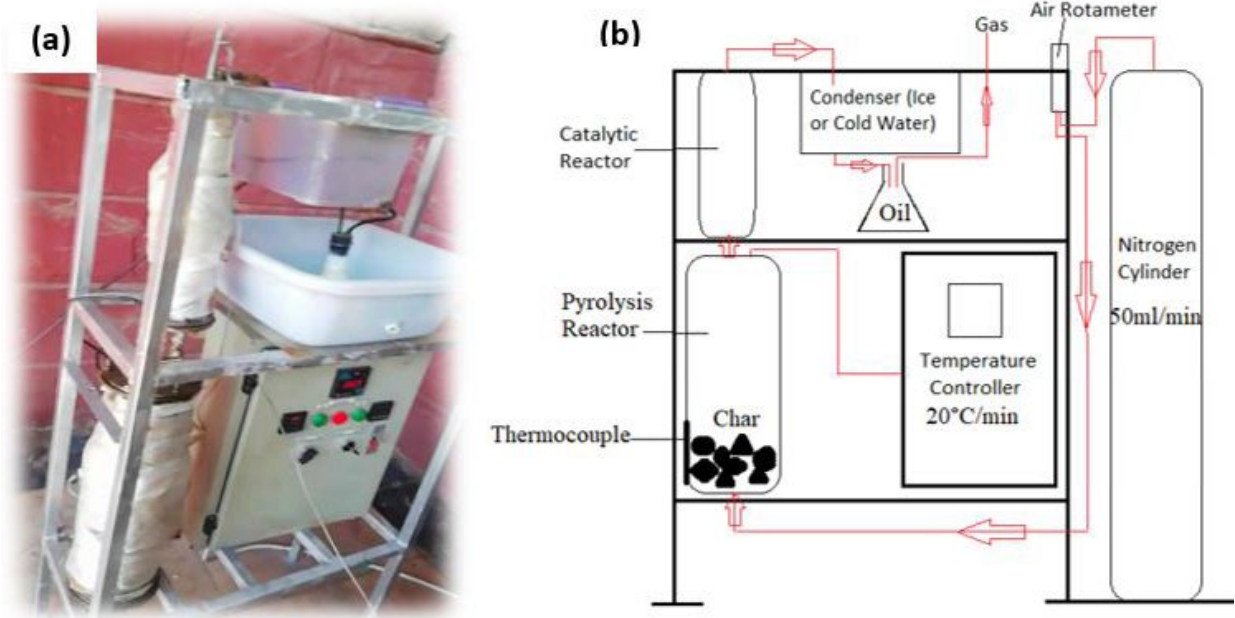


Fig. 3. 2. (a) Pyrolysis set up (b) Schematic Diagram of Pyrolysis

At the end of the procedure, the resultant biochar (BC), which is the feedstock's residue, was gathered. After the high-temperature oil and gas extraction, it was still within the pyrolysis reactor. Weighing the biochar with a gram-sensitive balance allowed us to determine its weight. Bagasse produced a yield of biochar that was higher than previously reported yields, at around 43.5%[56]. A Particle Size Analyzer (PSA) was used to measure the biochar's particle size. The biochar was constantly pounded in a mortar and pestle for 2 and 1/2 hours to further reduce the particle size, and the particle size was then analysed, as shown in Fig. 3. 3.



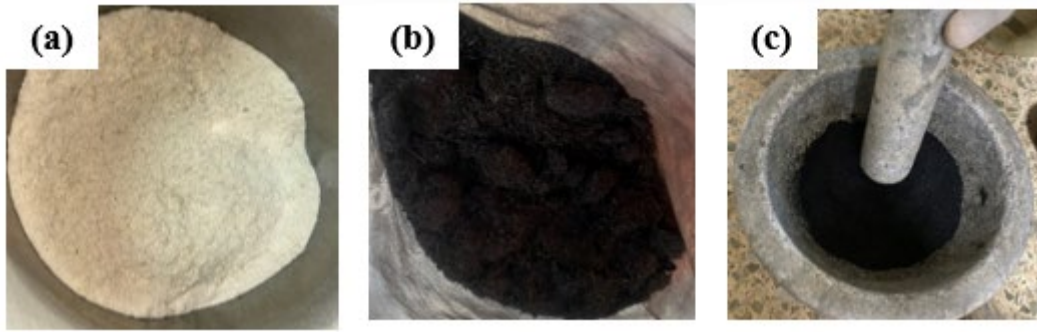


Fig. 3. 3. (a) Ground Bagasse (b) Biochar (c) Hand Grinding of Biochar

### 3.3.3 Bagasse Carbon Nano/Micro Particles

The pyrolysis procedure produced the powdered form of CNMPs. Ball milling was done for 150 minutes in order to get a nano-sized powder as shown in Fig. 3. 4. With a 1:20 ratio of milling medium to powder, the milling jar was filled to 25% of its optimum capacity. After the ball milling process, the particle size was determined by analyzing the Particle Size Distribution. Additionally, the particles' form and other characteristics were studied and characterized.

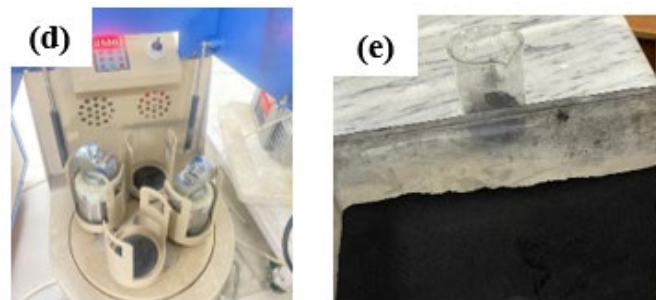


Fig. 3. 4. (d) Planetary ball milling of biochar (e) Milled Biochar (CNMPs)

## 3.4 Characterizations of bagasse CNMPs

Surface morphology, crystalline structure, micro/nano structure, elemental content, and functional groups of the CNMPs samples were all characterized.

### 3.4.1 Particle Size Distribution (PSD)

Using the "HORIBA Laser Scattering Particle Size Distribution Analyzer LA-920," laser granulometry was used to find out the particle sizes of CNMPs after ball milling.

### 3.4.2 Scanning Electron Microscopy and Energy Dispersive X-ray spectroscopy

With the use of the "TESCAN VEGA3" device and the SEM (Scanning Electron

Microscope) method, CNMPs and concrete samples' surface morphology and particle sizes were examined. Furthermore, Energy Dispersive X-ray (EDX) analysis was used to determine the elemental composition.

### **3.4.3 X-Ray Diffraction (XRD)**

X-ray Diffraction (XRD) analysis was used to carefully examine the structural composition, crystal/grain size, dislocation density, and micro stresses of CNMPs in order to obtain high accuracy. The measurements were carried out using a "Burker D8 Advance" apparatus that has a  $k\text{-}\alpha$  1 diffractometer. The investigation was carried out using high flux radiations throughout a  $2\theta$   $20^\circ$ - $80^\circ$  temperature range.

### **3.4.4 Thermal Gravimetric Analysis (TGA)**

Using a nitrogen environment, a Thermogravimetric Analysis (TGA) was performed to assess the thermal stability of CNMPs. The CNMPs were heated to a temperature range of  $0$ - $800^\circ\text{C}$ , with the temperature increasing at a rate of  $10^\circ\text{C}$  per minute, for the analysis.

### **3.4.5 Fourier Transform Infrared (FTIR)**

Fourier Transform Infrared Spectroscopy (FTIR) study of CNMPs was carried out using the "PerkinElmer Spectrum 100 FT-IR Spectrometer". This investigation included a spectrum ranging from  $400$  to  $4000\text{ cm}^{-1}$  and was focused on finding the surface functional groups present in CNMPs.

## **3.5 Mix proportions and preparation of CNMP's reinforced concrete samples**

Six varying concrete formulations were produced and summarized in Table 3-4. Following several experiments, the controlled recipe which has  $0\%$  CNMPs was particularly developed to reach a specified compressive strength of  $30\text{ MPa}$  at  $28$  days. The other five formulations each included bagasse CNMPs in increasing amounts, ranging from  $0.2\%$  by weight of cement to  $0.4\%$ ,  $0.6\%$ ,  $0.8\%$ , and  $1\%$ . A constant water-to-cement ratio of  $0.4$  was kept across all six mixes, and each recipe included  $1\%$  superplasticizer by weight of cement to ensure adequate workability.

Table 3- 4: Composition of concrete samples

Notation	CNMP'S	
	%age	Grams
0%CNMP's	0	0
0.2%CNMP's	0.2	30.508
0.4%CNMP's	0.4	61.018
0.6%CNMP's	0.6	91.524
0.8%CNMP's	0.8	122.032
1%CNMP's	1.0	152.54

Concrete examples were made using the materials indicated before. In order to encourage better cement hydration, a water-to-binder ratio (w/c) of 0.4 was used in the concrete mix ratio of 1:1.25.:1.5 (Cement: Fine Aggregates: Coarse Aggregates) [1]. A superplasticizer called "Chemrite 303" was added to improve workability at a dose of 1% in relation to the cement composition. For 45 minutes, sonication was used to ensure that the matrix was distributed evenly. Table 3-5 provides information on the size and number of samples generated from each batch.

Table 3- 5: No. and size of samples prepared from each batch.

Tests	Sample size	No of samples	ASTM standard
Freeze-thaw test	150mmx150mmx150mm	3	CEN/TS 12390-9
Chloride migration test	100mmx50mm	3	NT-BUILD 492
Compression test before freeze-thaw	100mmx100mmx100mm	3	ASTM C39
Compression test after freeze-thaw	100mmx100mmx100mm	3	ASTM C39
Acid attack	100mmx100mmx100mm	3	ASTM C-267

At the start, 500ml of water and 16.67g of nano/micro biochar were mixed together and sonicated for 45 minutes. The mixing water was then filled with this suspension. Cement, fine aggregates, and coarse aggregates were then added, and a 3-minute dry mixing period was completed. After that, the CNMPs suspension was added to the mixer, and more mixing was done for a further 2 minutes. As a result, the total mixing time was 5 minutes. In accordance with the recipe shown in Table 3-5, the resultant mixture was poured into cube moulds of conventional sizes, namely 150mm, 100mm cubes and 100mm cylinders cubes. After that, the samples underwent a dry curing process in the moulds for 24 hours at a temperature of 20 degrees Celsius. The samples were then cured for a total of 28 days in a curing tank.

### 3.6 Freeze-thaw testing

#### 3.6.1 Scaling

The CEN/TS 12390-9 standard was followed in order to conduct the frost scaling measurement[24]. The concrete mixture was poured into the moulds, and they were left to cure for 24 hours to produce 150mm-sized cube samples. The cubes were removed from the moulds after the allotted time had passed and placed in tap water that was kept at a constant temperature of  $20 \pm 2$  °C. The freeze-thaw test was started when the cubes were taken out of the water and transported to a climate chamber at the age of 7 days. A  $50 \pm 2$ mm thick specimen was cut at the age of 21 days, perpendicular to each cube's top surface, as shown in Figure 3-2.

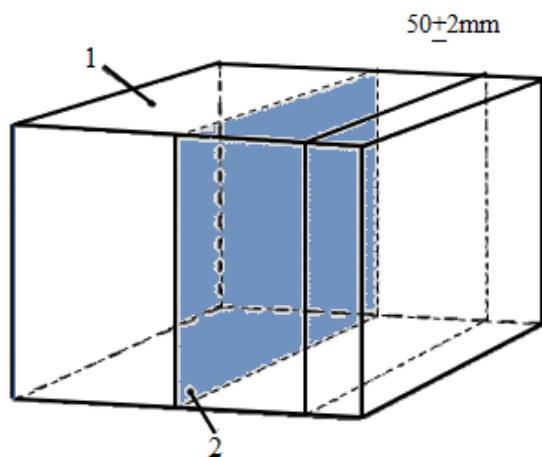


Figure 3-2: The test specimen and test surface are located in the sawn cube

1. Top surface at casting
2. Test surface

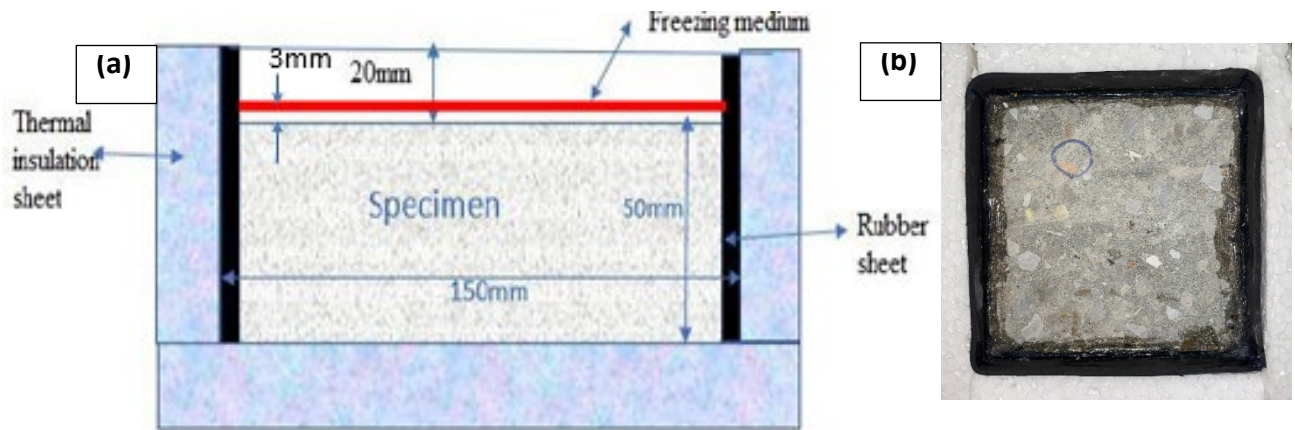


Fig. 3. 5. (a) The test arrangement (b) Prepared sample

The specimens were sliced, cleaned, and then transported right away to the climatic room. Rubber coverings were applied to all surfaces except the specified test surface after the specimens attained an age of  $25 \pm 1$  days, in accordance with the recommended methodology. The test surface was determined to be the sawn surface. Rubber sheets were placed with their edges reaching 20mm above the surface, and silicon was used to seal the gaps between the concrete and rubber sheets.

A thin coating of de-ionized water, about 3mm thick, was carefully placed to the surface of the specimens after the 28-day curing period. About 67ml of water were used to fill the 150mm x 150mm surface area to the appropriate depth of 3mm. The specimens were then left submerged in water for three days until the freeze-thaw test was conducted. The specimens were covered with an insulating sheet before the test was run in order to assure thermal insulation, with the exception of the defined test surface as shown in Fig. 3. 5. In a freeze-thaw chamber, samples were placed, and the temperature was controlled using the preprogrammed settings listed in Table 3-6. Any scaling material that had formed on the samples after 7, 14, 21, and 28 freeze-thaw cycles was gently brushed off. The removed scaling material was then fully dried by being heated to a temperature of  $105^{\circ}\text{C}$  while following the guidelines outlined in CEN/TS 12390-9. The dried scaling material was then measured in grams per square metre ( $\text{g}/\text{m}^2$ ) and weighed.

Table 3- 6: Time and temperature maintained during freeze-thaw cycle.

Upper limit		Lower limit	
Time (hours)	Temp (°C)	Time (hours)	Temp (°C)
0	+24	0	+16
5	-3	3	-5
12	-15	12	-22
16	-18	16	-22
18	-1	20	-1
22	+24	24	+16

### 3.6.2 Freeze- thaw Internal structure damage

The previously scaled specimens were used to assess the internal structural damage (ISD). ISD measurements were made using Ultrasonic Pulse Velocity Testing (UPVT), in accordance with CEN/TR 15177:2006[27], at 0, 7, 14, 21, and 28 cycles. Following the directions in the handbook, the ultrasonic equipment was precisely calibrated. To guarantee appropriate contact between the transducers and the indicated places on the specimens, a little quantity of sonic grease was applied. Once a stable minimum value was attained, the transducers were forcefully pushed against the concrete surface once more. Then, Equation 1 was utilised to calculate the Relative Dynamic Modulus (RDM).

$$RDM = (t_0/t_n)^2 \times 100[\%] \quad (\text{Equation 1})$$

Where;

RDM is relative dynamic modulus of elasticity in %

$t_0$  is initial transit time in microseconds

$t_n$  is transit time after n freeze-thaw cycles in microseconds

### 3.6.3 Compression test before and after freeze-thaw cycles

Followed by 28 freeze-thaw cycles at a loading rate of 0.1kn/sec, the compression test was carried out on 100mm cubes, as shown in the figure. For each formulation, three samples were examined before any freeze-thaw cycles were performed, and three samples were evaluated following the completion of 28 cycles of freeze-thaw. Following the ASTM C39 [28] testing technique, a total of 30 samples were examined.

### 3.7 Acid attack:

The acid resistance test was carried out in accordance with ASTM C-267's instructions [29]. For each formulation, three samples with dimensions of 100 mm x 100 mm x 100 mm were used. The use of 5% sulfuric acid solution was made. The concrete cubes were thoroughly saturated by being immersed in distilled water for three days prior to immersion, and their weights were noted. The cubes were then put in glass containers with the appropriate acidic solutions for a period of 28 days. The containers were covered throughout testing to reduce evaporation.

Each specimen was retrieved, brushed, and washed with distilled water to remove any scaled material after 14 and 28 days of immersion. The samples were then weighed again. By calculating the weight loss percentage using the formula:  $\text{weight loss (\%)} = [(W_o - W_i) / W_o] \times 100\%$  (Equation 2), the acid resistance was determined.

$$\text{weight loss (\%)} = [(W_o - W_i) / W_o] \times 100\% \quad (\text{Equation 2})$$

In this context,  $W_o$  stands for the specimen's initial weight in grams before being submerged in the acid solution, and  $W_i$  for the specimen's weight in grams following  $i$  days of immersion.

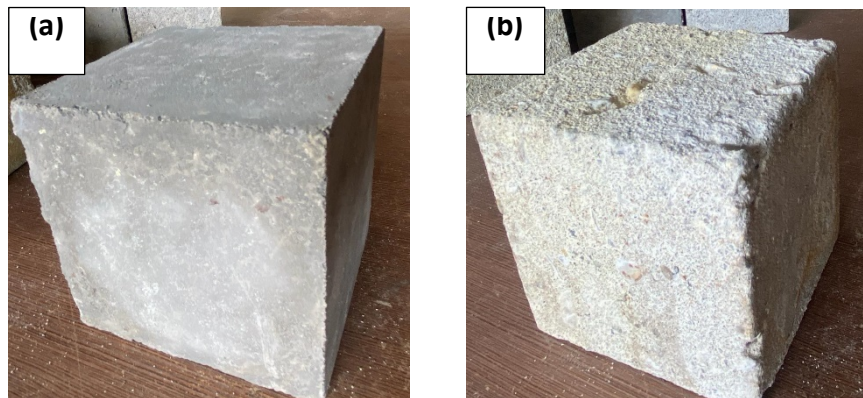


Fig. 3. 6. Specimen (a) before sulfate attack (b) after sulfuric attack

### 3.8 Chloride migration test:

On concrete specimens measuring 100x50 mm, the chloride migration test was conducted in compliance with the guidelines provided in NT Build 492. Evaluation of the non-steady state migration coefficient ( $D_{nssm}$ ) for each of the four mixtures was the goal of this test. Figure 3.16 (a)–(c) shows the photos that were taken throughout the test.

The specimens were carefully cleaned and washed after being sawn in order to get rid of any loose debris. The specimens were put into a vacuum container for further processing once their surfaces had dried. The pressure within the hoover container was kept between 1 to 5 KPa. Three hours of vacuum treatment were given to the samples, and then a solution of Ca(OH)<sub>2</sub> was added to completely immerse them all. Another hour was spent under the hoover. The specimens were then submerged in the solution for a further 18 hours before air was progressively added back into the container.

The experimental procedure followed the instructions outlined in the recommended test method NT-BUILD 492. 0.3M NaOH solution was used as anolyte reservoirs while 12 liters of a 10% NaCl solution was used in the catholyte reservoir. The power supply's positive terminal was attached to the anode, while its negative terminal was attached to the cathode. The initial current flowing through each item was carefully measured and recorded when a 60V voltage was introduced. The anolyte solution's starting temperature was also precisely measured. The final temperature and current readings were recorded for further study after a certain amount of time.

From Equation 3, the chloride migration coefficient was calculated..

$$D_{nssm} = \frac{0.0239(273+T)L}{(U-2)t} \left[ (x_d - \frac{0.0238\sqrt{(273+T)x_d}}{\sqrt{(U-2)}}) \right] \quad (\text{Equation 3})$$

Where:

$D_{nssm}$ : non-steady-migration co-efficient, x 10<sup>-12</sup>m<sup>2</sup>/sec;

U: Absolute of applied voltage, V

T: average value of initial and final temperatures in anolyte solution OC

L: thickness of specimen, mm

X<sub>d</sub>: average value of penetration depths, mm

t: test duration, hour



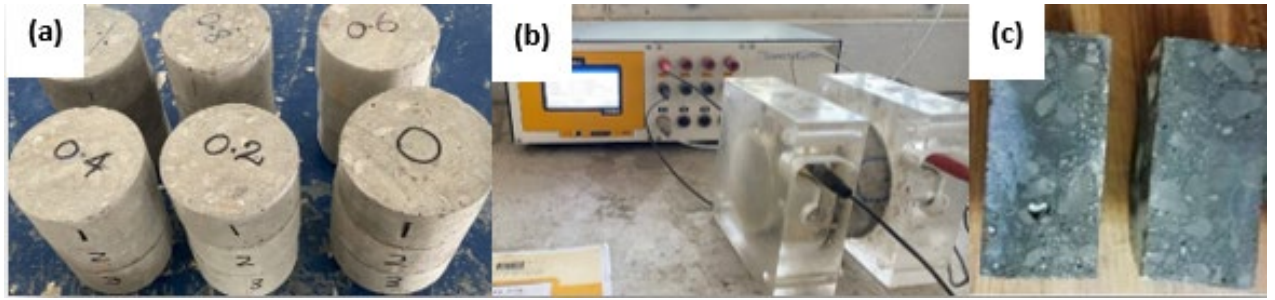


Fig. 3. 7. Chloride Migration Test

### 3.9 Microstructural investigation

For further investigation in the study, the specimens were collected. These extracted specimens, which were around 5 to 10 mm in size, were ready for Brunauer-Emmett-Teller (BET) and scanning electron microscopy (SEM) investigation. The samples underwent an initial phase of drying in an oven at 50°C for a duration of 24 hours in order to speed up the testing procedure. After then, the hydration process was stopped by submerging the samples in acetone for a further 24 hours. With the help of Scanning Electron Microscope, the specimens were analyzed for Interfacial Transition Zone (ITZ), microstructure, crack bridging, and crack control. The pore sizes and volumes were determined using BET analysis. The specimens' interior porosity was also examined in order to evaluate the impact of CNMP.

## 4 RESULTS AND DISCUSSION

### 4.1 Characterization of bagasse CNMPs

The following studies have been done to assess the morphology, nano/microstructure, crystallinity, and content of bagasse CNMPs.

#### 4.1.1 Particle Size Distribution (PSD)

The cumulative passing % and the average particle size of particles in the biochar samples before grinding (BG) and after grinding (AG) were evaluated using the laser granulometry method. The 20mg CNMPs were sonicated in 200ml of distilled water before being submitted to the particle size distribution (PSD) assessment. This sonication procedure made sure that the particles were well distributed and made it easier to quantify the precise particle sizes, as shown in Fig. 4. 1.

The test outcomes show that the D50 values of BC were 27.7 $\mu\text{m}$  and 5.58 $\mu\text{m}$ , respectively, before and after grinding, while the D90 values were 116.2 $\mu\text{m}$  and 8.81 $\mu\text{m}$ , respectively. The particle size analyzer, however, was unable to identify particles in the nano size range, according to the cumulative CNMP's percentage curve. This finding suggested the potential existence of nanoparticles, which was further validated by characterization methods using SEM and XRD.

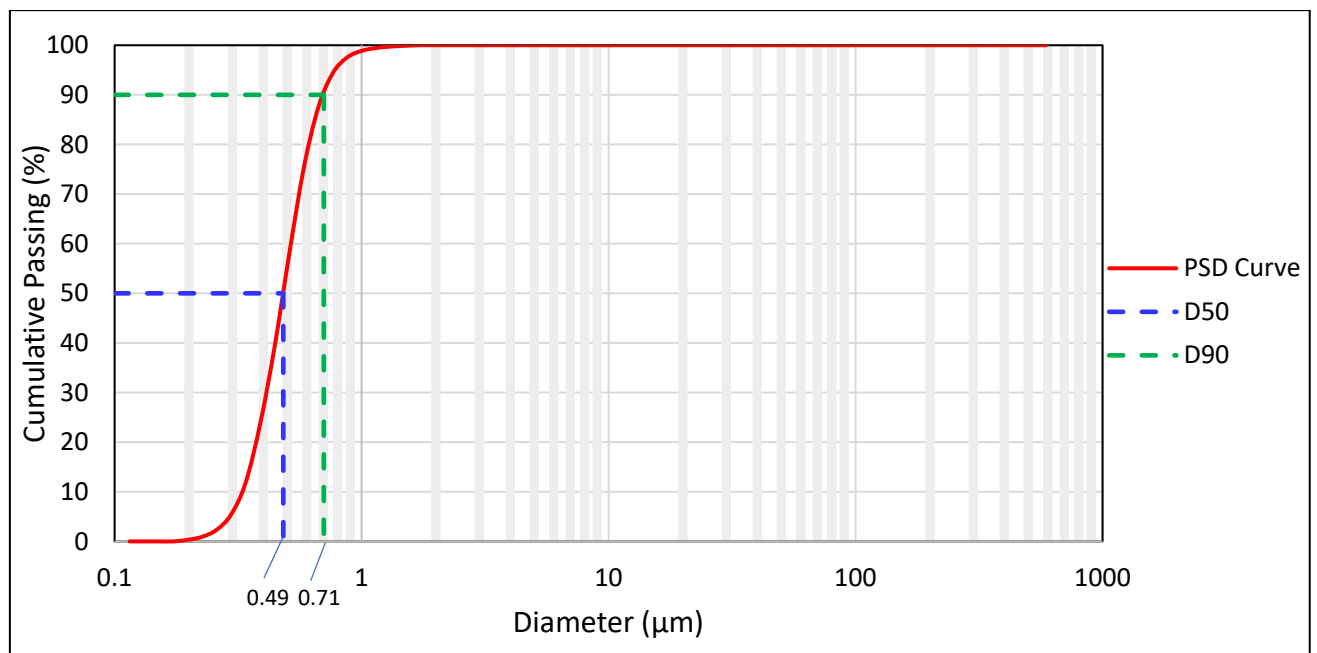


Fig. 4. 1. Particle size distribution of bagasse CNMPs

#### 4.1.2 Scanning Electron Microscopy (SEM) and EDX

The surface texture, particle size, and morphology of CNMPs were evaluated by SEM inspection. As seen in Fig 4. 2 (a), the SEM micrographs obtained showed that CNMPs has an irregular form and is characterized by sheet-like structures rather than discrete particles. The sheets were discovered to have an average width of  $4\mu\text{m}$  and a thickness of around  $1\text{ metres}$ . As shown in Fig. 4. 2 (b), it was discovered that upon closer inspection, these sheets include embedded nano-sized particles with an average size of around  $100\text{ nm}$ .

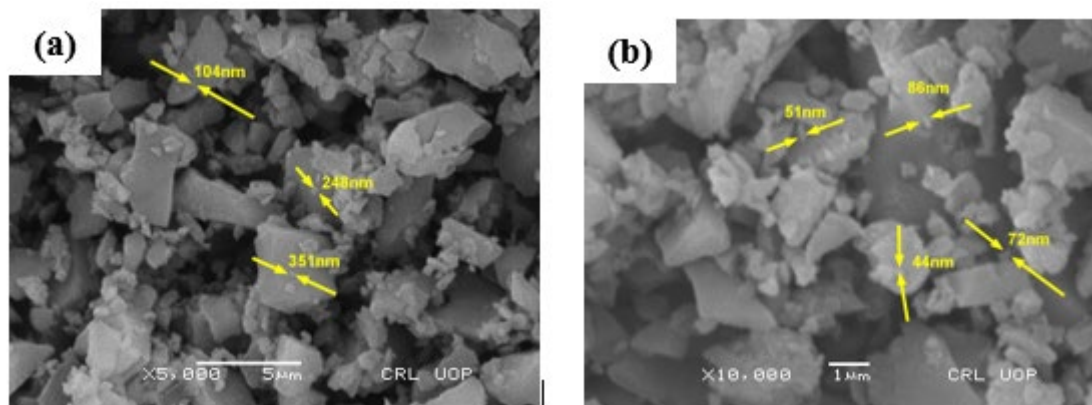


Fig. 4. 2. (a) SEM image of bagasse CNMP sheets (b) Nano Particles embedded in sheets  
As shown in Figure 4.3 and summarized in Table 4.1, an EDX analysis was carried out on a chosen spectrum point within the SEM image. Finding the sample's weight % composition was the goal of this analysis. The findings showed that carbon, with a value of  $90.67\%$ , comprised the biggest percentage by weight. This result adds to the evidence that the carbon in CNMP was produced through the pyrolysis process. It is significant that oxygen may be found in CNMP since it was absorbed from the atmosphere around it.

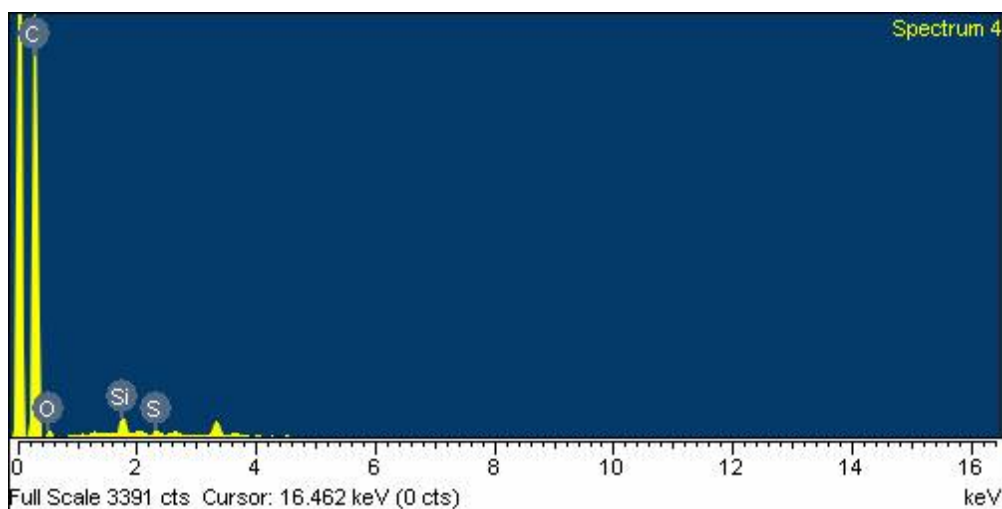


Fig. 4. 3. EDX Spectra of bagasse CNMP

Table 4- 1: Composition of bagasse CNMP

C (weight %)	O (weight %)	Ca (weight %)
90.67	7.60	1.24

The CNMPs does not include impurities like Fe, Mg, Al, P, K, and others. Therefore, it can be said that its purity level is higher than many earlier research[57].

#### 4.1.3 X-Ray Diffraction (XRD)

Grazing incidence X-ray diffraction (GIXRD) investigation utilising a Bruker AXS: D8 Discover instrument was used to look at the structural features of the produced CNMP. We used Cu K $\alpha$  radiation with a wavelength of 0.154 nm and a step width of 0.02°. The diffraction pattern of CNMPs in the 2 range of 20° to 80° is depicted by the XRD pattern in Fig. 4. 4. The crystal structure of the minerals sucrose (H12C22O11), chromium (Cr), and calcite (CaCO<sub>3</sub>), respectively, are (-2 2 0), (1 1 0), and ( 3 0 0) at 2 values of 26.38°, 44.07°, and 68.47°, respectively.

Debye-Scherrer's equation[58] was used to calculate the density of dislocations and the average size of CNMP's crystallites, which results in equations (4.1) and (4.2). The findings showed that the dislocation density was 0.00205 nm<sup>-2</sup> (equal to 2.05x10<sup>-12</sup> m<sup>-2</sup>), with an average crystallite size of 22.86 nm. The number of dislocations indicates if there are flaws in the crystalline particles [127, 128].

$$D = \frac{0.97\lambda}{\beta \cos \theta} \quad (4.1)$$

$$\delta = \frac{1}{D^2} \quad (4.2)$$

The micro lattice strain of CNMPs was calculated using the Williamson-Hall technique [129], which produced a result of 0.001691 as shown by equation (4.3).

$$\text{Strain } (\varepsilon) = \frac{\beta \cos \theta}{4} \quad (4.3)$$

Previous studies by Hatcher et al. (1996) and Chen et al. (2016), who also noted similar position in close vicinity to the mentioned angle, provided further proof of the existence

of calcite, supporting the results obtained in this study.

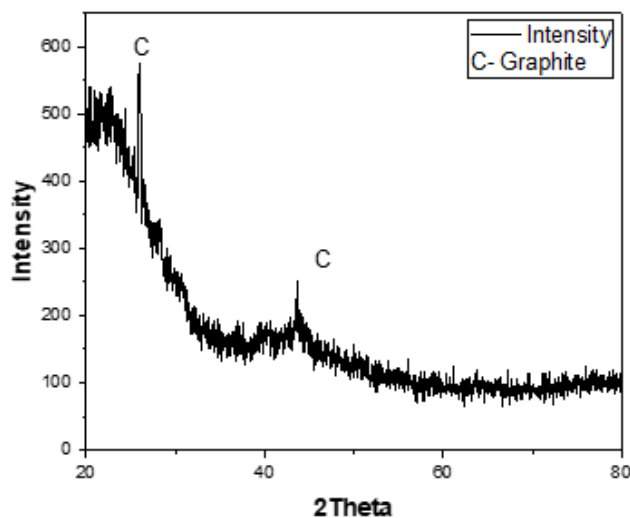


Fig. 4. 4. X-Ray Diffraction pattern of CNMPs

#### 4.1.4 Fourier Transform Infrared Spectroscopy (FTIR)

Fourier transform infrared (FTIR) spectrometer with a gold-coated integrating sphere and an 8° angle of incidence was used to examine the vibrational properties of CNMP. A number of absorption bands matching to resonant frequencies were seen in the 400–4000  $\text{cm}^{-1}$  spectral region. The unique bond or functional group present in the sample is represented by each peak in the FTIR spectrum[59]. In particular, the C-H bonding vibrations[60] or the out-of-plane deformation of this functional group[59] are responsible for a peak at 875  $\text{cm}^{-1}$  wavenumber. The presence of alcohol and ester groups in the CNMP sample is shown by peaks at 1114.5  $\text{cm}^{-1}$  and 1429.5  $\text{cm}^{-1}$  that are linked to C-O and C-H bonds.

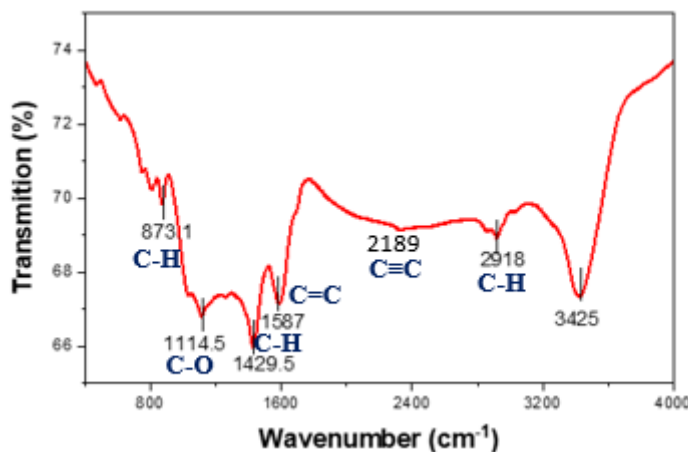


Fig. 4. 5. FTIR spectra of CNMPs

The peak found at 1587  $\text{cm}^{-1}$ [61], which denotes the creation of carbonized material during the pyrolysis process, confirmed the existence of C=C aromatic groups. The stretching vibrations of the C-O bond are represented by a large and asymmetric peak at 1701  $\text{cm}^{-1}$ , which raises the possibility of the presence of numerous C-O functional groups, including anhydrides, ketones, and carboxylic acids ester[62]. Similar to the broad peak at 2190  $\text{cm}^{-1}$ , C-C stretching modes are most likely responsible to ester's weak[61]. Alkyl C-H groups are linked to the peaks seen at 2917  $\text{cm}^{-1}$  [134]. Furthermore, the peak at 3421  $\text{cm}^{-1}$  suggests that lignocellulosic components have been dehydrated [135, 136]. These findings offer convincing proof that biochar has been produced from bagasse sugarcane.

#### 4.1.5 Thermal Gravimetric Analysis (TGA)

Thermal gravimetric analysis (TGA) was used to evaluate the synthetic biochar's thermal stability. As shown in Figure 4.8, TGA measurements were performed by gradually rising the temperature from 0°C to 800°C at a rate of 1°C per minute.

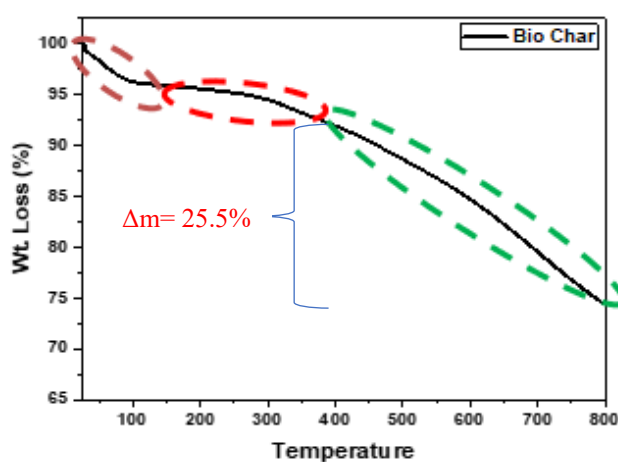


Fig. 4. 6. TGA plot of biochar

The temperature versus mass loss graph shows that a significant mass loss was seen between two separate temperature ranges: 0°C to 100°C and 400°C to 800°C. Between 0°C and 100°C Moisture removal is responsible for the early exothermic mass loss curve, whereas permanent carbon combustion or the start of carbonization through volatile matter evaporation are responsible for the subsequent mass loss. By the time the temperature hit 800°C, up to 25.5% of the mass had been lost, and no more mass loss was seen after that. The presence of non-combustible ash components has been shown by a

linear trend in the TGA plot. It's noteworthy that the ash content of the biochar was discovered to be lower than results previously reported[63]. These TGA results demonstrate the product's remarkable stability under high temperatures. Experimental research was carried out in compliance with relevant standards, and the results are discussed in this chapter. The focus of this chapter is on analyzing how CNMPs affect the durability and strength of nano-modified concrete. To find various performance, many experiments were conducted. All studies were conducted in a highly controlled laboratory environment with a constant room temperature of 20°C and a carefully controlled humidity level of at least 65%. The results are arranged into two primary categories: Mechanical and Durability properties, and Microstructure analysis.

## **4.2 Freeze-thaw testing in concrete**

### **4.2.1 Scaling**

By incorporating CNMPs and utilizing the Slab test method from CEN/TS 12390-9[64], the freeze-thaw scaling of the concrete was investigated. After 7, 14, 21, and 28 freeze-thaw cycles, the concrete's scaling was evaluated. The control mixture without CNMPs showed very high scaling, exceeding the CEN/TS 12390-9 scaling criterion for concrete (1000 g/m<sup>2</sup>). As shown in Fig. 4. 7, it has been discovered that adding CNMPs to the concrete mixture considerably reduces freeze-thaw scaling. By enhancing the material's microstructure, the inclusion of CNMPs has led to scaling reductions of up to 75%. By enhancing packing, strengthening the interfacial transition zone, and creating solid connections with the matrix through van der Waals forces, CNMPs significantly contribute to the modification of the structure[65]. Additionally, because of their distinctive form, CNMPs may efficiently block and reroute microcracks, which slows down crack development.

The results of the SEM study support the microstructure's densification, which was made possible by the presence of hydration products and the obstruction and diversion of cracks by both hydration products and CNMPs. Figure 4-3 (a) indicates a lower concentration of hydration products, whereas Fig. 4. 8(b) demonstrates a considerable increase in hydration products because of the CNMPs particles intrusion. The nucleation sites on CNMPs, which facilitate the precipitation of hydration products, are responsible for this rise. Additionally, the calcium silicate hydrate (CSH) gel, in particular, covers all of the

particles, resulting in a decrease in total porosity. The interior microstructure's higher strength and lower permeability as a result of the better density reduce water absorption and scaling effects. The results of the SEM study support the microstructure's densification, which was made possible by the presence of hydration products and the obstruction and diversion of cracks by both hydration products and CNMPs. Figure 4-3 (a) indicates a lower concentration of hydration products, whereas Fig. 4. 8(b) demonstrates a considerable increase in hydration products because of the CNMPs particle intrusion. The nucleation sites on CNMPs, which facilitate the precipitation of hydration products, are responsible for this rise. Additionally, the calcium silicate hydrate (CSH) gel, in particular, covers all of the particles, resulting in a decrease in total porosity. The interior microstructure's greater strength and lower permeability as a result of the better density reduce water absorption and scaling effects.

A substantial rise in the air content results with an inclusion of nanomaterials, especially in the range of 0-0.3%[66]. The CNMPs used in our study also have nanoparticles that function as entrainment agents for air, increasing the quantity of air in the matrix. This increased air content is essential for reducing freeze-thaw scaling. Other researchers have looked at the use of nanomaterials to improve freeze-thaw resistance in a number of studies. For instance, research on carbon nanotubes (CNTs) has shown that introducing them improves freeze-thaw resistance by improving porosity, lowering permeability, and enabling fracture bridging[67].

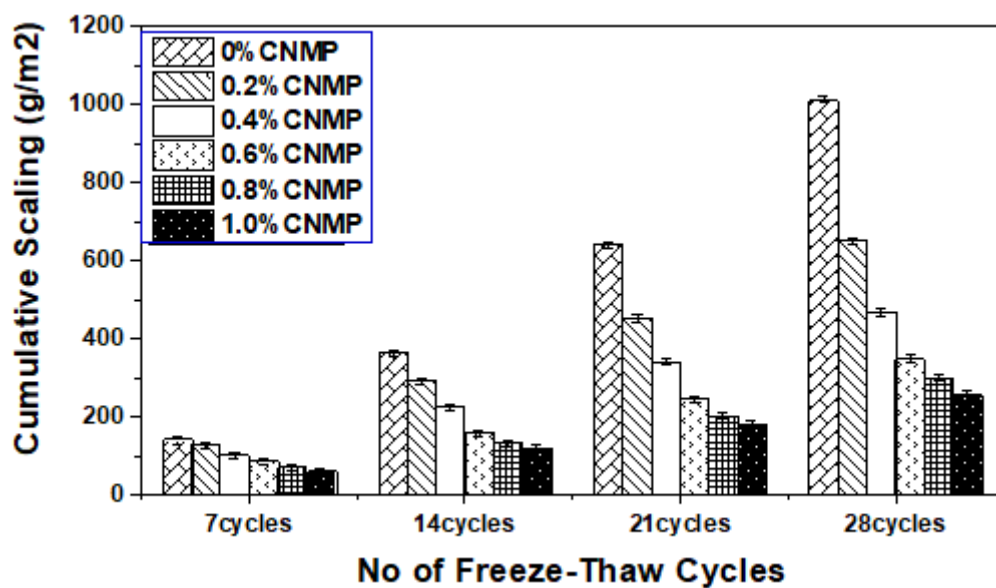


Fig. 4. 7. Freeze-thaw scaling



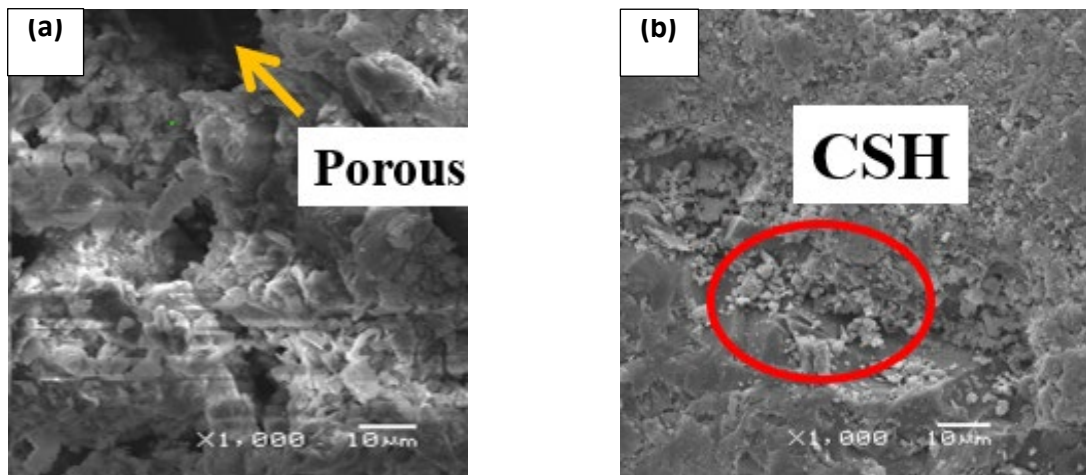


Fig. 4. 8. SEM images of (a) 0%CNMP's (b) 1%CNMP's before freeze-thaw cycles

#### 4.2.2 Freeze-thaw internal structure damage

In order to assess the damage triggered by freeze-thaw cycles on the inner structure of concrete, CNMPs were added using the Slab test procedure CEN/TR 15177[64]. Through the use of an ultrasonic pulse transit time test, the degree of internal structural damage was identified. The Resilient Dynamic Modulus (RDM) of Elasticity was calculated using the test measurements, and the findings are shown in Fig. 4. 9. Internal structural damage (ISD) was lowered as a result of the inclusion of CNMPs as the nanomaterial enhanced gel pores while decreasing capillary pores. Due to internal microcracks, freeze-thaw exposure often results in increase in the total porosity of concrete. The total number of gel pores is a key factor in determining the degree of internal structural damage, since more gel pores lead to less damage. Furthermore, the freeze-thaw cycle is more likely to cause damage to small pores. Water in bigger capillary pores freezes before water in smaller capillary pores when both are exposed to freeze thaw action. The water in gel pores, on the other hand, is kept at a much lower temperature and only freezes when the outside temperature falls below -78 degrees Celsius[64].

The amount of water in the concrete is significantly decreased when CNMPs are added to the mix to reduce its permeability. This decrease in water content causes the osmotic pressure to drop, which lessens the harm imposed by freezing. SEM analysis supports the finding that the damage decreased with the addition of CNMPs. The formation of microcracks as a result of freeze-thaw cycles is seen in Fig. 4. 10(a). Larger fractures and more extensive deterioration were observed in the samples containing less amount

of CNMPs. In Fig. 4. 10(b), on the other hand, the presence of CNMPs in the dense microstructure denotes a lower level of degradation, and the sheets like structure of CNMPs prevents fracture propagation or alters their direction.

The relationship with reduced permeability and improved resistance to freeze-thaw cycles has been explored in a number of studies[14]. The mixture comprises more air due to the presence of carbon nano/micro particles. Because of this, formulations with more air frequently exhibit less interior structural damage.

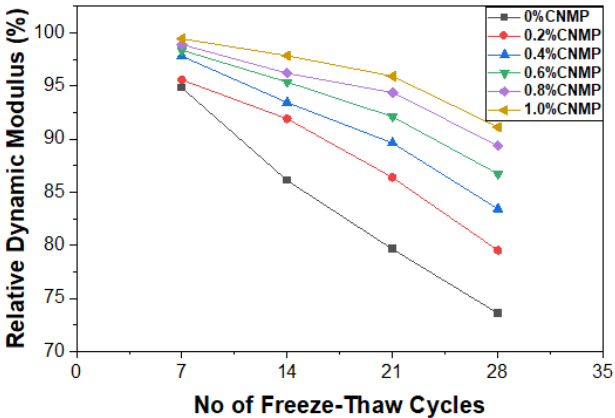


Fig. 4. 9. Internal structure damage

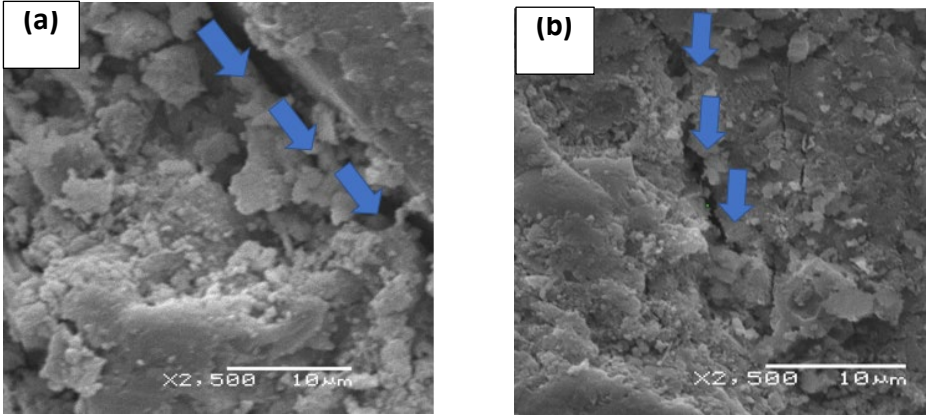


Fig. 4. 10. Scanning electron microscopy of (a) 0%CNMP's (b) 1%CNMP's after frost attack

**4.2.3 Compression test before and after freeze-thaw cycles**

The outcomes of the experiments clearly show a correlation between increased compressive strength and the addition of CNMPs. This can be understood by the fact that CNMPs have an elastic modulus that is noticeably greater than that of concrete, leading to an overall increase in compressive strength. A load is transferred to the contact between

the cement matrix and CNMPs when it is applied. In comparison to the interface between cement and aggregates, the contact incorporating CNMPs can withstand a larger load, ultimately leading to an overall gain in strength. The development of the interfacial transition zone and the bridging effect caused by microcracks are responsible for the improvement in compressive strength.

CNMPs, show improved load resistance after breaking. This is explained by the fact that they have a higher surface area, which encourages the development of more hydrates in the mixture and hence raises compressive strength[28]. Compressive strength significantly increases with the addition of CNMPs. However, the percentage increment was reduced due to the re-agglomeration of CNMPs at greater dosages, resulting in the formation of poor sites. This may be the reason for this minor change in trend. According to studies, adding CNMPs improves mortar's compressive strength. Similar to this, Kumar et al. found that the incorporation of CNTs (Carbon Nanotubes) increased compressive strength, but at greater concentrations, agglomeration resulted in a loss in strength. The use of nanoparticles improved compressive strength. Additionally, it has been discovered that the addition of carbon fibres causes the compressive strength to improve substantially by 20–50%. According to the results, CNMPs should make up 0.8% of a material in order to achieve the greatest compressive strength. After 28 freeze-thaw cycles, the compressive strength of the combination with CNMPs exhibited a loss of only 9.5% as opposed to a fall of 35% for the mixture without CNMPs. These findings clearly show the beneficial effects of CNMPs in enhancing the concrete durability.

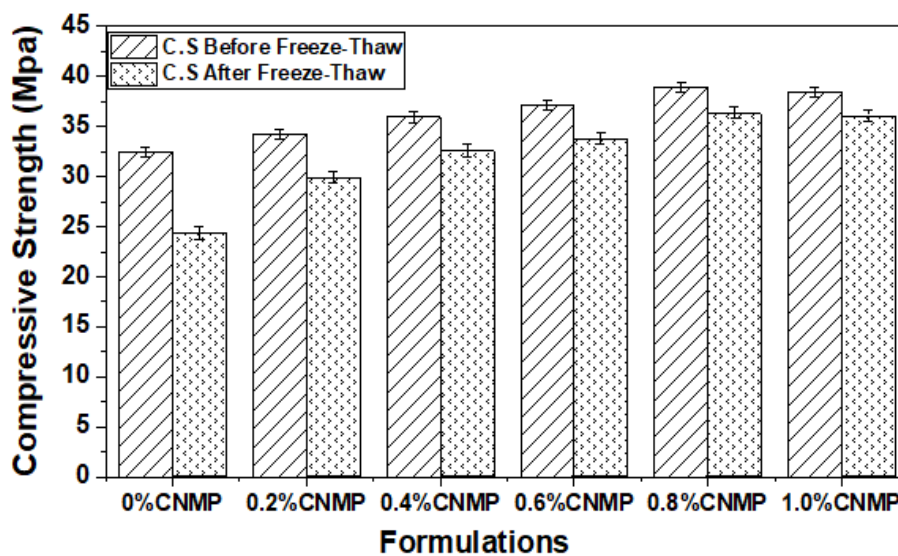


Fig. 4. 11. Comparison of compressive strength before and after freeze-thaw cycles

### 4.3 Acid attack in concrete

Due to its alkaline characteristics, concrete is prone to deterioration when exposed to acids. Concrete's composition may be harmed by acidic chemicals. An acid attack test was performed to determine how different concrete formulations performed under conditions with high acid concentration. Concrete samples were submerged in 5% sulfuric acid for 14 and 28 days, respectively. By evaluating how much weight loss the samples underwent, the resilience of the concrete mixtures was evaluated. Fig. 4 depicts the weight loss of the control and CNMP mixtures followed by exposure. With an increase in CNMP concentration, weight loss diminishes for sulfuric acid attacks. The microstructure of the mix grows denser, and the permeability reduces as the fraction of CNMP's increases. Therefore, when the amount of CNMP in the mixture increases, the water absorption increases. This means that a rise in the proportion of CNMPs causes a decrease in the absorption of acid, which prevents degradation and weight loss. Consequently, the reduction in weight loss may be caused by the existence of a thick microstructure. After 28 days of exposure to sulfuric acid, the 1%CNMPs and 0%CNMPs mixes of concrete showed the min and max weight loss, with values of 2.71% and 6.5%, accordingly. Based on the results, it can be said that sulfuric acid has a greater negative impact on the degradation of concrete. Ettringite is produced as a result of the interaction between sulfuric acid and concrete, which causes the latter to expand and fracture. Additionally, the inclusion of MWCNTs was shown to improve sulphate resistance. The efficient packing of MWCNTs at the nano- and microscales, which lowered permeability, is responsible for this improvement. The enhanced performance is also due to the nanomaterial's higher mechanical characteristics. Another important factor in preventing the fractures at the beginning and spread is the homogeneous distribution of MWCNTs across the mixture [40].

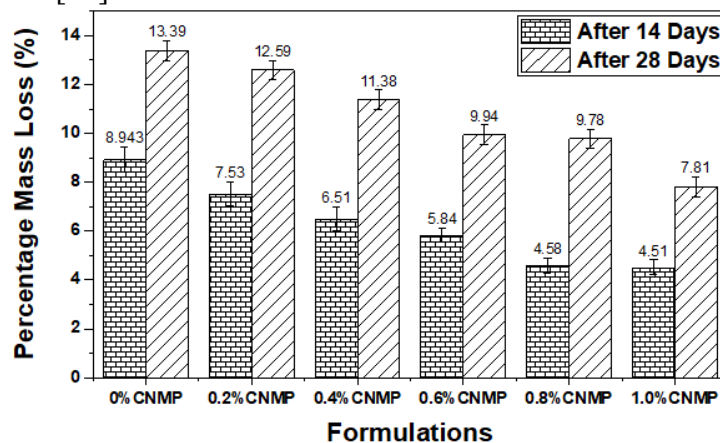


Fig. 4. 12. Sulfate attack scaling at 14 and 28 days exposure

#### **4.4 Chloride migration test in concrete**

Corrosion of reinforcement is one of the main causes of concrete degradation, essentially by the migration of chloride ions. The durability of building is substantially impacted by the rate at which chloride ions permeate through the concrete. The corrosion process commences when chloride ions get close to the reinforcing bars. The NT-BUILD 492 test method is used to assess the concrete's ability to withstand chloride penetration and its durability against chloride-induced degradation. To calculate the chloride migration coefficient, which acts as a gauge of the material's resistance to chloride ion penetration, non-steady-state migration experiments are used in this test process.

According to Table 4-2, the findings of the chloride migration test reveal that specimens with increased CNMPs contents exhibit improved immunity to entry of chloride. Equation 3 is used to compute the migration coefficient values by taking the depth of chloride penetration into consideration. As was previously said, figuring out the migration coefficient, as shown in Fig. 4. 13, is crucial to assessing the chloride resistance parameter. This can be explained by the development of a more compact and impermeable concrete structure as a result of the inclusion of CNMPs.

The diffusion rate of chloride ions was decreased as a result of the integration of CNMPs due to a considerable reduction in porosity. Through BET and SEM measurements, this reduction in porosity and the matrix's densification were validated. According to published research, alterations in the pore structure can affect concrete's resistance to chloride penetration[44]. Additionally, Carbon Nanotubes (CNTs) have demonstrated that by minimizing porosity and pore size, they can improve the resistance to chloride penetration[49]. Similar to MWCNTs, MWCNTs' strong mechanical characteristics, nano- and micro-sized packing, and resistance to chloride penetration have contributed to this resistance. Fracture initiation and propagation are prevented by the homogenous distribution of Nano materials within the mixture.

Table 4- 2: Penetration depth and migration co-efficient

Sample type	Penetration depth (mm)	Migration coefficient, D <sub>snm</sub> (10 <sup>-12</sup> m <sup>2</sup> /sec)
0%CNMP's	17.5	8.91
0.2%CNMP's	13.4	6.67
0.4%CNMP's	11.1	5.43
0.6%CNMP's	8.3	3.94
0.8%CNMP's	6.4	2.94
1%CNMP's	5.7	2.57

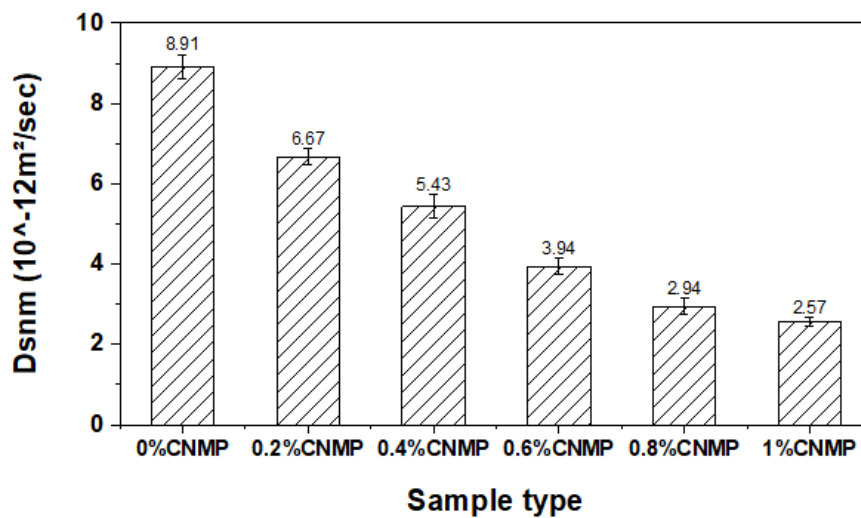


Fig. 4. 13. Chloride migration co-efficient

#### 4.5 BET Porosimetry in concrete

The BET test method is often employed to calculate the accurate surface area of porous materials and can be used instead of MIP to determine the distribution of pores. However, it is important to understand that the pre-treatment method selected might affect the outcomes of BET analysis. Several techniques are used during the pre-treatment stage to remove free water from the sample. Oven drying, D-drying, and methanol exchange

following D-drying are the three key techniques. It is important to remember that various pre-treatment strategies might provide a range of results. High temperatures must be avoided while using oven drying since they might lead to the disintegration of CSH gel and a partial collapse of the void structure. As a result, the sample underwent a 24-hour pre-treatment at 60°C. The strategies indicated above and their influence on outcomes have been investigated.

As illustrated in Fig. 4. 14, a rise in relative pressure indicates that more nitrogen is absorbed in the sample, indicating that the pore volume of the concrete has been decreased as a result of the CNMP intrusion. The figure shows that after 28 freeze-thaw cycles, the sample's relative pressure has grown, but that the sample with graphite platelets has experienced far less impact than the control sample. Fig. 4. 14 illustrates the distribution of pore sizes. Both before and after frost attack, the addition of CNMPs causes refinement in the pore size and pore volume. Prior to and after frost attack, the pore volume reveals reductions of up to 32% and 34%, respectively. The addition of CNMPs to concrete has been shown in earlier experiments to increase the mixture's porosity. Other nanomaterials, such as CNTs, have also been shown to have favorable impacts on microstructure improvement and porosity reduction, according to a number of studies[68]. Notably, the presence of MWCNTs has resulted in a remarkable porosity reduction of up to 64% [48].

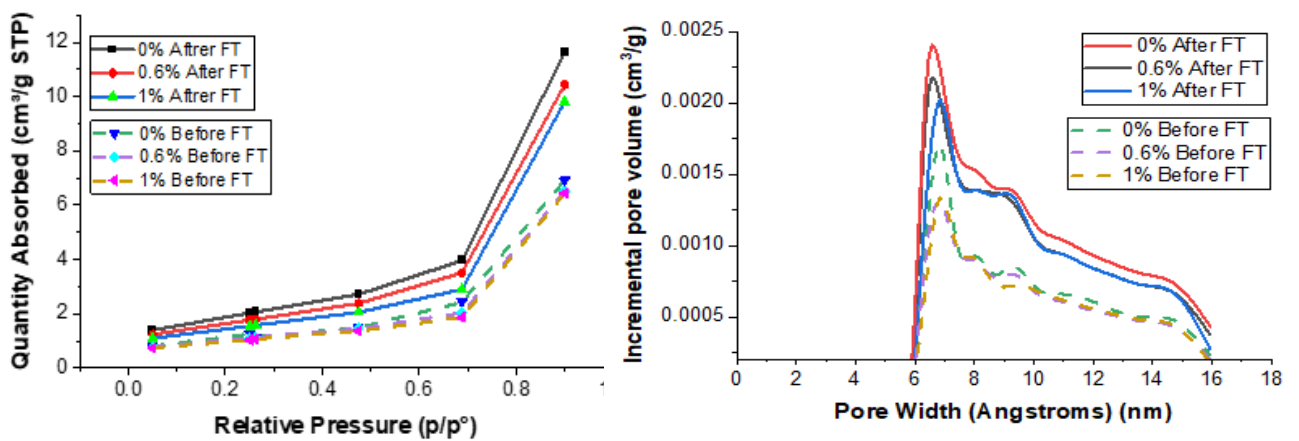


Fig. 4. 14. Nitrogen absorption isotherm (a) before (b) after frost attack

### 5 CONCLUSIONS AND RECCOMENDATIONS

#### 5.1 Conclusions

- The findings of this work provide new perspectives into the durability and performance features of concrete treated with nanomaterials. The following conclusions have been made on the basis of the investigations.
  
- Micro-nano size carbonized bagasse has been prepared successfully by pyrolysis process, the product is chemically and thermally stable.
- The results of the SEM and BET analyses indicate that, considerable reduction in porosity and the development of a compact microstructure, resulting in a mixture that is extremely impermeable.
- The compressive strength of the mixture is noticeably improved with the incorporation of well-dispersed CNMPs. Additionally, when 1% graphite platelets are added, the detrimental effect of freeze-thaw cycles on compressive strength is reduced from 24.96% to 6.63%.
- The stamina of the concrete matrix to salt freeze-thaw scaling is improved with the addition of CNMPs, and the degree of improvement is directly related to the quantity of GNMPs employed. The salt freeze-thaw scaling decreases as much as 74.42% by adding 1% graphite platelets.
- As shown by the BET data, the concrete mix containing 1% CNMPs had the best resilience to changes in porosity brought on by Internal Structure Damage. Additionally, compared to the control mix, the SEM study showed less internal structural damage, which is likely due to the CNMPs' ability to bridge and pin cracks.
- The drop in weight loss from 13.39% to 7.81% was noted when subjected to sulfuric acid which indicates that the concrete's acid resistance has increased.
- Along with chloride penetration, chloride migration coefficient have decreased as a result of the drop in permeability. While the migration coefficient was reduced by as much as 71.15%, the penetration of chloride was diminished by 67.42%.
- Consequently, CNMPs were successfully incorporated into the cementitious matrix in this study to improve its , microstructure, durability and strength.



## **5.2 Recommendations**

- It is advised to incorporate CNMPs into concrete at concentrations exceeding 1% in order to evaluate the point at which their effectiveness begins to diminish with respect to durability.
- The utilization of SCMs (Supplementary Cementitious Materials) in conjunction with these nanoparticles, and their impact on freeze-thaw resistance, acid attack, and chloride penetration, should be considered.

## REFERENCES

- [1] M. Safiuddin, U. J. Alengaram, M. M. Rahman, M. A. Salam, and M. Z. Jumaat, "Use of recycled concrete aggregate in concrete: A review," *J. Civ. Eng. Manag.*, vol. 19, no. 6, pp. 796–810, 2013, doi: 10.3846/13923730.2013.799093.
- [2] A. André, J. De Brito, A. Rosa, and D. Pedro, "Durability performance of concrete incorporating coarse aggregates from marble industry waste," *J. Clean. Prod.*, vol. 65, pp. 389–396, 2014, doi: 10.1016/j.jclepro.2013.09.037.
- [3] S. Frondistou-Yannas, "Waste Concrete as Aggregate for New Concrete," *ACI J. Proc.*, vol. 74, no. 8, doi: 10.14359/11019.
- [4] J. W. Bullard and J. Schweitzer, "Mechanisms of Cement Hydration," no. December 2017, 2011, doi: 10.1016/j.cemconres.2010.09.011.
- [5] *Fifth Edition.*
- [6] N. P. Kim, L. V. C., and K. Toshiro, "Fracture Toughness of Microfiber Reinforced Cement Composites," *J. Mater. Civ. Eng.*, vol. 14, no. 5, pp. 384–391, Oct. 2002, doi: 10.1061/(ASCE)0899-1561(2002)14:5(384).
- [7] P. W. Zhu, P. J. M. Bartos, and A. Porro, "Application of nanotechnology in construction Summary of a state-of-the-art report," no. September, 2014, doi: 10.1007/BF02483294.
- [8] F. Babak, H. Abolfazl, R. Alimorad, and G. Parviz, "Preparation and Mechanical Properties of Graphene Oxide: Cement Nanocomposites," *Sci. World J.*, vol. 2014, p. 276323, 2014, doi: 10.1155/2014/276323.
- [9] K. S. Novoselov, A. K. Geim, S. V Morozov, and D. Jiang, "Electric Field Effect in Atomically Thin Carbon Films," vol. 306, no. October, pp. 666–669, 2004.
- [10] S. Ahmad, G. A. Ferro, L. Restuccia, J. M. Tulliani, and P. Jagdale, "Materials and Mix Proportions," vol. 34, pp. 534–542, 2015, doi: 10.3221/IGF-ESIS.34.59.
- [11] J. Njuguna, "Structural Nanocomposites Perspectives for Future Applications."
- [12] D. Nulty, M. Kiley, and N. Meyers, "Promoting and recognising excellence in the supervision of research students: An evidence-based framework," *Assess. Eval. High. Educ.*, vol. 34, no. 6, pp. 693–707, 2009, doi: 10.1080/02602930802474193.
- [13] S. Gupta and H. Kua, "Effect of water entrainment by pre-soaked biochar particles on strength and permeability of cement mortar," *Constr. Build. Mater.*, vol. 159, Oct. 2017, doi: 10.1016/j.conbuildmat.2017.10.095.
- [14] J. Li, P.-S. Wong, and J.-K. Kim, "Hybrid nanocomposites containing carbon nanotubes

- and graphite nanoplatelets,” *Mater. Sci. Eng. A*, vol. 483–484, pp. 660–663, 2008, doi: <https://doi.org/10.1016/j.msea.2006.08.145>.
- [15] “K Rahal mechanical prop of conc with RCA.pdf.” .
- [16] P. Zhu, Y. Hao, H. Liu, D. Wei, S. Liu, and L. Gu, “Durability evaluation of three generations of 100% repeatedly recycled coarse aggregate concrete,” *Constr. Build. Mater.*, vol. 210, pp. 442–450, Jun. 2019, doi: 10.1016/j.conbuildmat.2019.03.203.
- [17] H. S. B. and S. A. M., “Mechanical and Freeze-Thaw Durability Properties of Recycled Aggregate Concrete Made with Recycled Coarse Aggregate,” *J. Mater. Civ. Eng.*, vol. 27, no. 10, p. 4015003, Oct. 2015, doi: 10.1061/(ASCE)MT.1943-5533.0001237.
- [18] S. Kannan, K. Arunachalam, and D. Brindha, “Performance analysis of recycled aggregate concrete with chemical admixture,” *Struct. Concr.*, vol. 22, Feb. 2020, doi: 10.1002/suco.201900380.
- [19] P. Matar and J. Barhoun, “Effects of waterproofing admixture on the compressive strength and permeability of recycled aggregate concrete,” *J. Build. Eng.*, vol. 32, p. 101521, 2020, doi: <https://doi.org/10.1016/j.jobe.2020.101521>.
- [20] S. Kou, C. Poon, and F. Agrela, “Comparisons of natural and recycled aggregate concretes prepared with the addition of different mineral admixtures,” *Cem. Concr. Compos.*, vol. 33, no. 8, pp. 788–795, 2011, doi: <https://doi.org/10.1016/j.cemconcomp.2011.05.009>.
- [21] P. Amorim, J. De Brito, and L. Evangelista, “Concrete made with coarse concrete aggregate: Influence of curing on durability,” *ACI Mater. J.*, vol. 109, no. 2, pp. 195–204, 2012, doi: 10.14359/51683706.
- [22] A. Chaipanich, T. Nochaiya, W. Wongkeo, and P. Torkittikul, “Compressive strength and microstructure of carbon nanotubes–fly ash cement composites,” *Mater. Sci. Eng. A*, vol. 527, no. 4, pp. 1063–1067, 2010, doi: <https://doi.org/10.1016/j.msea.2009.09.039>.
- [23] G. Y. Li, P. M. Wang, and X. Zhao, “Mechanical behavior and microstructure of cement composites incorporating surface-treated multi-walled carbon nanotubes,” *Carbon N. Y.*, vol. 43, no. 6, pp. 1239–1245, 2005, doi: <https://doi.org/10.1016/j.carbon.2004.12.017>.
- [24] G. Sun, R. Liang, Z. Lu, J. Zhang, and Z. Li, “Mechanism of cement/carbon nanotube composites with enhanced mechanical properties achieved by interfacial strengthening,” *Constr. Build. Mater.*, vol. 115, pp. 87–92, 2016, doi: <https://doi.org/10.1016/j.conbuildmat.2016.04.034>.

- [25] T. Nochaiya and A. Chaipanich, “Behavior of multi-walled carbon nanotubes on the porosity and microstructure of cement-based materials,” *Appl. Surf. Sci.*, vol. 257, pp. 1941–1945, Jan. 2011, doi: 10.1016/j.apsusc.2010.09.030.
- [26] A. Naqi, N. Abbas, N. Zahra, A. Hussain, and S. Q. Shabbir, “Effect of multi-walled carbon nanotubes (MWCNTs) on the strength development of cementitious materials,” *J. Mater. Res. Technol.*, vol. 8, no. 1, pp. 1203–1211, 2019, doi: <https://doi.org/10.1016/j.jmrt.2018.09.006>.
- [27] B. Wang, Y. Han, and S. Liu, “Effect of highly dispersed carbon nanotubes on the flexural toughness of cement-based composites,” *Constr. Build. Mater.*, vol. 46, pp. 8–12, 2013, doi: <https://doi.org/10.1016/j.conbuildmat.2013.04.014>.
- [28] A. Sobolkina *et al.*, “Dispersion of carbon nanotubes and its influence on the mechanical properties of the cement matrix,” *Cem. Concr. Compos.*, vol. 34, no. 10, pp. 1104–1113, 2012, doi: <https://doi.org/10.1016/j.cemconcomp.2012.07.008>.
- [29] S. Ahmad, R. Khushnood, P. Jagdale, J.-M. Tulliani, and G. Ferro, “High performance self-consolidating cementitious composites by using micro carbonized bamboo particles,” *Mater. Des.*, vol. 76, Jul. 2015, doi: 10.1016/j.matdes.2015.03.048.
- [30] S. Xu, J. Liu, and Q. Li, “Mechanical properties and microstructure of multi-walled carbon nanotube-reinforced cement paste,” *Constr. Build. Mater.*, vol. 76, pp. 16–23, 2015, doi: <https://doi.org/10.1016/j.conbuildmat.2014.11.049>.
- [31] B. B. Mukharjee and S. V Barai, “Influence of Nano-Silica on the properties of recycled aggregate concrete,” *Constr. Build. Mater.*, vol. 55, pp. 29–37, 2014, doi: <https://doi.org/10.1016/j.conbuildmat.2014.01.003>.
- [32] L. P. Singh, S. Karade, S. Bhattacharyya, M. M. Yousuf, and S. Ahalawat, “Beneficial role of nanosilica in cement based materials – A review,” *Constr. Build. Mater.*, vol. 47, Oct. 2013, doi: 10.1016/j.conbuildmat.2013.05.052.
- [33] M. N. Muhd Sidek, M. S. Hamidah, and M. Arshad, “Applications of using nano material in concrete: A review,” *Constr. Build. Mater.*, vol. 133, pp. 91–97, Feb. 2017, doi: 10.1016/j.conbuildmat.2016.12.005.
- [34] Y. Reches *et al.*, *Development of Nano-Modified Concrete for Next Generation of Storage Systems report*. 2018.
- [35] L. P. Singh, S. R. Karade, S. K. Bhattacharyya, M. M. Yousuf, and S. Ahalawat, “Beneficial role of nanosilica in cement based materials - A review,” *Constr. Build. Mater.*, vol. 47, pp. 1069–1077, 2013, doi: 10.1016/j.conbuildmat.2013.05.052.
- [36] A. Heidari and D. Tavakoli, “A study of the mechanical properties of ground ceramic

- powder concrete incorporating nano-SiO<sub>2</sub> particles,” *Constr. Build. Mater.*, vol. 38, pp. 255–264, Jan. 2013, doi: 10.1016/j.conbuildmat.2012.07.110.
- [37] S. Parveen, S. Rana, and R. Fanguero, “A Review on Nanomaterial Dispersion, Microstructure, and Mechanical Properties of Carbon Nanotube and Nanofiber Reinforced Cementitious Composites,” *J. Nanomater.*, vol. 2013, Jan. 2013, doi: 10.1155/2013/710175.
- [38] B. Huang, “Carbon nanotubes and their polymeric composites : the applications in tissue engineering,” *Biomanufacturing Rev.*, vol. 5, no. 1, pp. 1–26, 2020, doi: 10.1007/s40898-020-00009-x.
- [39] B. Wang, B. Wang, L. Yan, Q. Fu, and B. Kasal, “A Comprehensive Review on Recycled Aggregate and Recycled Aggregate Concrete Resources , Conservation & Recycling A Comprehensive Review on Recycled Aggregate and Recycled Aggregate Concrete,” *Resour. Conserv. Recycl.*, vol. 171, no. May, p. 105565, 2021, doi: 10.1016/j.resconrec.2021.105565.
- [40] P. Zhan, J. Xu, J. Wang, J. Zuo, and Z. He, “A review of recycled aggregate concrete modified by nanosilica and graphene oxide : Materials , performances and mechanism,” *J. Clean. Prod.*, vol. 375, no. June, p. 134116, 2022, doi: 10.1016/j.jclepro.2022.134116.
- [41] H. M. Allujami, M. Abdulkareem, T. M. Jassam, R. A. Al-Mansob, J. L. Ng, and A. Ibrahim, “Nanomaterials in recycled aggregates concrete applications: mechanical properties and durability. A review,” *Cogent Eng.*, vol. 9, no. 1, 2022, doi: 10.1080/23311916.2022.2122885.
- [42] Z. Luo, W. Li, V. W. Y. Tam, J. Xiao, and S. P. Shah, “Current progress on nanotechnology application in recycled aggregate concrete,” *J. Sustain. Cem. Mater.*, vol. 8, no. 2, pp. 79–96, 2019, doi: 10.1080/21650373.2018.1519644.
- [43] M. T. Hasholt, *Air void structure and frost resistance : A challenge to Powers ’ spacing factor*, no. May 2014. 2015.
- [44] N. Salemi, K. Behfarnia, and S. A. Zaree, “Effect of nanoparticles on frost durability of concrete,” *Asian J. Civ. Eng.*, vol. 15, pp. 411–420, Jun. 2014.
- [45] K. Tan and J. Nichols, “Frost Resistance of Concrete with Different Strength Grades and Mineral Admixtures,” *Mod. Civ. Struct. Eng.*, vol. 1, Dec. 2017, doi: 10.22606/mcse.2018.21001.
- [46] “NRC Publications Archive Archives des publications du CNRC,” 1976.
- [47] N. Salemi, K. Behfarnia, and S. A. Zaree, “Effect of nanoparticles on frost durability of concrete,” *Asian J. Civ. Eng.*, vol. 15, no. 3, pp. 411–420, 2014.

- [48] C. Carbon *et al.*, “Investigation on the Mechanical Properties of a Cement-Based Material Investigation on the Mechanical Properties of a Cement-Based Material Containing Carbon Nanotube under Drying and Freeze-Thaw Conditions,” no. December, 2015, doi: 10.3390/ma8125491.
- [49] X. Wang, I. Rhee, Y. Wang, and Y. Xi, “Compressive Strength , Chloride Permeability , and Freeze-Thaw Resistance of MWNT Concretes under Different Chemical Treatments,” vol. 2014, 2014.
- [50] ASTM C136, “ASTM C136/C136M Standard Test Method for Sieve Analysis of Fine and Coarse Aggregates,” *ASTM Stand. B.*, no. January, pp. 3–7, 2019, doi: 10.1520/C0136.
- [51] A. ASTM, “C128 e 15 Standard test method for relative density (specific gravity) and absorption of fine aggregate. West Conshohocken,” *ASTM Int. West Conshohocken PA*, vol. i, p. ASTM C128 e 15, 2015, doi: 10.1520/C0128-15.2.
- [52] ASTM C127, “Standard Test Method for Density, Relative Density (Specific Gravity), and Absorption of Coarse Aggregate,” *Annu. B. ASTM Stand.*, pp. 1–5, 2004, doi: 10.1520/C0127-15.2.
- [53] IS : 2386 (Part IV ), “Methods of test for Aggregates for Concrete, part 4 : Mechanical properties,” *Bur. Indian Stand. New Delhi*, pp. 1–37, 2016.
- [54] N. Ahmed, M. Zeeshan, N. Iqbal, M. Z. Farooq, and S. A. Shah, “Investigation on bio-oil yield and quality with scrap tire addition in sugarcane bagasse pyrolysis,” *J. Clean. Prod.*, vol. 196, pp. 927–934, 2018, doi: <https://doi.org/10.1016/j.jclepro.2018.06.142>.
- [55] A. K. Sakhiya, A. Anand, V. K. Vijay, and P. Kaushal, “Thermal decomposition of rice straw from rice basin of India to improve energy-pollution nexus: Kinetic modeling and thermodynamic analysis,” *Energy Nexus*, vol. 4, no. November, p. 100026, 2021, doi: 10.1016/j.nexus.2021.100026.
- [56] S. G. C. de Almeida, L. A. C. Tarelho, T. Hauschild, M. A. M. Costa, and K. J. Dussán, “Biochar production from sugarcane biomass using slow pyrolysis: Characterization of the solid fraction,” *Chem. Eng. Process. - Process Intensif.*, vol. 179, no. February, 2022, doi: 10.1016/j.cep.2022.109054.
- [57] E. Ahmad, N. Jäger, A. Apfelbacher, R. Daschner, A. Hornung, and K. K. Pant, “Integrated thermo-catalytic reforming of residual sugarcane bagasse in a laboratory scale reactor,” *Fuel Process. Technol.*, vol. 171, pp. 277–286, 2018, doi: <https://doi.org/10.1016/j.fuproc.2017.11.020>.
- [58] F. Leitão Muniz, M. Miranda, C. Morilla-Santos, and J. Sasaki, “The Scherrer equation

- and the dynamical theory of X-ray diffraction,” *Acta Crystallogr. Sect. A Found. Adv.*, vol. 72, May 2016, doi: 10.1107/S205327331600365X.
- [59] E. Ogunsona, A. Rodriguez, A. Mohanty, and M. Misra, “Mechanical , Chemical , and Physical Properties of Wood and Perennial Grass Biochars for Possible Composite Application,” no. February, 2016, doi: 10.15376/biores.11.1.1334-1348.
- [60] F. O. The, “Infrared spectroscopy absorption table,” pp. 1–7, 2015.
- [61] L. M. Costa, E. Siebeneichler, and J. Tronto, “Characterization of biochars from different sources and evaluation of release of nutrients and contaminants Characterization of biochars from different sources and evaluation of release of nutrients and contaminants 1,” no. July, 2017, doi: 10.5935/1806-6690.20170046.
- [62] C. H. Chia, B. Gong, S. D. Joseph, C. E. Marjo, P. Munroe, and A. M. Rich, “Imaging of mineral-enriched biochar by FTIR, Raman and SEM–EDX,” *Vib. Spectrosc.*, vol. 62, pp. 248–257, 2012, doi: <https://doi.org/10.1016/j.vibspec.2012.06.006>.
- [63] M. D. F. Salgado, A. M. Abioye, and M. Mat, “Preparation of activated carbon from babassu endocarp under microwave radiation by physical activation Preparation of activated carbon from babassu endocarp under microwave radiation by physical activation,” pp. 0–13, 2018.
- [64] S. Standard, “iTeh STANDARD PREVIEW iTeh STANDARD PREVIEW,” vol. 1, no. I, pp. 2–5, 2020.
- [65] W. Khaliq and M. B. Ehsan, “Crack healing in concrete using various bio influenced self-healing techniques,” *Constr. Build. Mater.*, vol. 102, pp. 349–357, 2016, doi: <https://doi.org/10.1016/j.conbuildmat.2015.11.006>.
- [66] V. Shubina, L. Gaillet, T. Chaussadent, T. Meylheuc, and J. Creus, “Biomolecules as a sustainable protection against corrosion of reinforced carbon steel in concrete,” *J. Clean. Prod.*, vol. 112, pp. 666–671, 2016, doi: <https://doi.org/10.1016/j.jclepro.2015.07.124>.
- [67] E. Rakanta, T. Zafeiropoulou, and G. Batis, “Corrosion protection of steel with DMEA-based organic inhibitor,” *Constr. Build. Mater.*, vol. 44, pp. 507–513, 2013, doi: <https://doi.org/10.1016/j.conbuildmat.2013.03.030>.
- [68] A. Cwirzen and K. Habermehl-Cwirzen, “The Effect of Carbon Nano- and Microfibers on Strength and Residual Cumulative Strain of Mortars Subjected to Freeze-Thaw Cycles,” *J. Adv. Concr. Technol.*, vol. 11, pp. 80–88, Mar. 2013, doi: 10.3151/jact.11.80.

